vious study, we observed an adaptive response in the lung of *gpt* delta mice treated with NNK, a tobacco specific nitrosamine, combined with γ-irradiation [9]. The methylating agent, i.e., NNK, significantly suppresses mutations induced by γ-irradiation in the lungs of mice. To explore the mechanisms underlying the apparent adaptive response, we examined combined effects of MNNG, a directly acting methylating agent, and γ-irradiation in the human lymphoblastoid cell lines TK6 and MT1 *in vitro* (Fig. 1). Single treatments of MNNG or γ-irradiation increased the frequencies of mutations, MN induction and cell death in both TK6 and MT1 (Figs. 2 and 3). In the combined treatments, however, induction of TK mutation, MN and cell death by γ-irradiation were significantly suppressed by pretreatments with MNNG not in MT1 but in TK6.

At first, we hypothesized that γ-induced apoptosis might be enhanced by the pretreatments with MNNG, thereby suppressing the mutations and MN induction in TK6 cells. However, the apoptosis was rather suppressed by the pretreatments with MNNG in TK6 cells (Fig. 4). No significant changes were observed in apoptosis in MT1 cells by the pretreatments. Suppression of radiation-induced apoptosis is known to be elicited by low-dose ionizing irradiation, which is called radioadaptive response [26–30]. Although the exact mechanism underlying the radioadaptive response is largely unknown, it is generally thought that cellular defense mechanisms against genotoxic effects of radiation are induced by prior exposure to low-dose radiation. Many of genes including p53, ATM and Chk1 are up- and down-regulated in the adapting cells [31]. Interestingly, we observed enhanced expression of p53 in MNNG-pretreated cells in the presence of MMR proteins (TK6) but not in the absence of them (MT1) (Fig. 5a). In fact, p53 is reported to play an important role in both apoptosis and DNA repair pathways depending on the level of DNA damage [22,23,32]. When cells are exposed to low or moderate levels of DNA damage, p53 does not induce apoptosis but activates error-free DNA repair, e.g., homologous recombination, thereby suppressing cell death. Therefore, we suggested that pretreatments with MNNG at low doses induce low or moderate levels of DNA damage and activate p53 in a way that it alleviates radiation-induced apoptosis. In this activation process, MMR proteins play crucial roles to mediate the signal from DNA damage to p53 (see below).

Because increased apoptosis was not the case, we next examined another possibility of whether MNNG pretreatments might delay cell-cycle progression, thereby acquiring resistance to genotoxicity of radiation. Intriguingly, when TK6 cells were treated with MNNG at a low dose, i.e., 1.5 ng/mL, the percentage of cells at G2/M was significantly increased (Table 1). No such increases were observed in TK6 cells treated with MNNG at a high dose, i.e., 150 ng/mL, or in MT1 cells treated with low or high doses of MNNG. Thus, we suggested that the activation of p53 by exposure to the low dose of MNNG suppresses cell cycle progression at G2/M phase, which in turn leads to enhanced error-free repair of DSBs in DNA. The enhancement of DNA repair at prolonged G2/M phase may account for the apparent adaptive response observed in TK6 cells (Fig. 6). This notion is supported by previous studies that indicate that treatments of cells with MNNG induce cell cycle delay at G2/M phase [18,33–35]. It is suggested that the MMR proteins interact with Ataxia telangiectasia mutated kinase (ATM) and ATM-and-Rad3-related kinase (ATR), thereby activating p53, Chk1 and cell cycle checkpoint proteins [21,36–38]. p38 activation is also reported to be important for methylating agent-induced G2 arrest in glioma and colon cancer cell lines [39]. In our case, however, Chk1 was not phosphorylated in both cell lines after MNNG pretreatments. This raises the possibility that Chk1 phosphorylation may not be necessary for cell cycle delay in TK6 cells. Alternatively, it is because we examined the phosphorylation of Chk1 by the Western blotting analysis earlier before it is detectably activated. Recently, Quiros et al. demonstrated that Chk1 was activated more effectively in the post-treatment cell cycle following O^6-methylguanine (O^6-MeG) induction treated by low concentration MNNG and suggested that

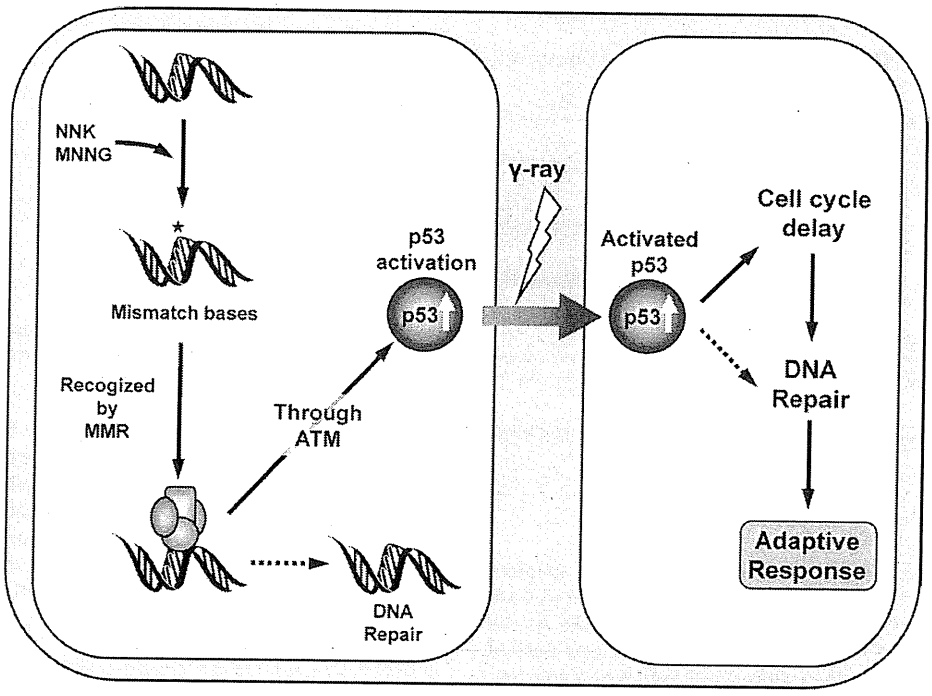

Fig. 6. A possible mechanism underlying the adaptive response of MNNG-pretreated TK6 cells against genotoxicity of γ-irradiation. Alkylating agents, i.e., NNK and MNNG, induce mismatch bases such as O^6-methylguanine paired with thymine in DNA, which are recognized by mismatch repair (MMR) proteins. After the recognition, the mismatch bases may be repaired by MMR in one pathway. In the other pathway, however, the mismatch-bound MMR recruits ATM and activates p53. The activation leads to cell cycle delay at G2/M and enhances error-free DNA repair, which results in induction of the adaptive response.

Chk1 activation requires at least two rounds of replication after the treatment of MNNG [40]. It is reported that MMR-dependent cell cycle arrest fully occurs after the second S-phase following DNA damage. We examined the Chk1 phosphorylation 24 h after the initiation of MNNG pretreatments when not all the cells might have finished the second round of DNA replication (Fig. 1). Unlike the checkpoint analysis, however, MN and gene mutations were analyzed 3 days after the termination of MNNG pretreatments. Hence, the cells replicated chromosome DNA in the presence of methylated damage, e.g., O^6-MeG, in DNA more than two times, which may be a reason why we observed clear suppressive effects against genotoxicity of γ-irradiation (Figs. 2 and 3). The results that we observed the suppressive effects 3 days after the MNNG pretreatments also raise a possibility that the adaptive response induced by MNNG may continue at least for 3 days.

The results in this study suggest that functional interactions of MMR proteins with p53 play critical roles in the adaptive response elicited by MNNG pretreatments (Fig. 6). Then, how does methylated DNA damage such as O^6-MeG induce activation of p53 via MMR proteins? One possibility is that a mismatch base-pair of O^6-MeG with thymine is recognized by MMR proteins, which in turn recruit other proteins, e.g., ATM, that stabilize and activate p53 [38]. Alternatively, the recognition of the mismatch base-pair by MMR proteins may lead to futile DNA synthesis, which results in generation of single-strand gaps and/or DSBs in DNA. These aberrant structures of DNA induce ATM, which can activate p53 and other proteins related to DNA damage response. Further work using mutant MMR proteins that can recognize the mismatch base-pairs but not interact with other proteins may give us insight into the roles of MMR proteins in induction of signals to p53.

It is evident that p53 activation leads to cell death via apoptosis when the DNA damage is severe. However, as described above, it is suggested that p53 activation leads to onset of DNA repair and enhancement of cell survival. Therefore, it is expected that there is a threshold below which p53 acts as a suppressor of cell death (or genotoxicity) and upon which p53 acts as an enhancer of cell death. Interestingly, suppression against radiation-induced genotoxicity was only observed at a specific dose of MNNG, i.e., 1.5 ng/mL for cell survival and TK gene mutations, and 1.5 and 3.0 ng/mL for MN induction (Figs. 2 and 3). Therefore, the dose responses of TK and MN assays were U-shaped along with the pretreatment doses of MNNG. These results may reflect the biphasic roles of p53 in cell survival (relief of genotoxicity) and cell death depending on the doses of MNNG. It is reported that severe DNA damage activates p53-independent apoptosis via p73, a protein homologous to p53 [41]. Because p73 is stabilized by MNNG treatments and silencing of p73 results in significant decreases in apoptosis and increases in survival, p73 appears to play a role in MMR-dependent apoptosis induced by MNNG treatment [42]. In this study, however, we could not observe enhanced apoptosis in TK6 cells pretreated with MNNG after γ-irradiation (Fig. 4). Thus, we suggest that apoptosis via p73 is not involved in the adaptive response in TK6 cells pretreated with MNNG against γ-irradiation (Figs. 2 and 3). It remains an open question, however, whether p73 may play a role in the adaptive response via other pathways, e.g., activation of DNA repair.

In summary, our results suggest that exposure to MNNG at low-doses induces adaptive response to radiation-induced genotoxicity in human cells and also that MMR proteins and p53 play critical roles in the adaptation. The results also suggest that the adaptive response depends on the priming dose of MNNG and perhaps the timing when the genotoxicity is analyzed. Obviously, further work is needed to thoroughly understand the mechanisms underlying the MNNG-induced adaptive response against radiation and how the mechanisms can be generalized to other combined genotoxicity of chemicals and radiation.

Conflict of interest

No conflict of interest.

Acknowledgements

We thank Dr. Masami Yamada (NIHS) for reading the manuscript carefully. Part of this study was financially supported by the Budget for Nuclear Research of the Ministry of Education, Culture, Sports, Science and Technology, based on the screening and counseling by the Atomic Energy Commission; grants-in-aid for scientific research from the Ministry of Education, Culture, Sports, Science and Technology, Japan [MEXT, 18201010; MEXT, 22241016]; the Ministry of Health, Labor and Welfare, Japan [H21-Food-General-009]; the Japan Health Science Foundation [KHB1007] and the Tutikawa Memorial Fund for Study in Mammalian Mutagenicity.

References

[1] Tobacco smoke and involuntary smoking, IARC Monogr. Eval. Carcinog. Risk Chem. Hum. 83 (2002).
[2] S.S. Hecht, Biochemistry, biology, and carcinogenicity of tobacco-specific N-nitrosamines, Chem. Res. Toxicol. 11 (1998) 559–603.
[3] S.S. Hecht, Tobacco carcinogens, their biomarkers and tobacco-induced cancer, Nat. Rev. Cancer 3 (2003) 733–744.
[4] R. Guza, M. Rajesh, Q. Fang, A.E. Pegg, N. Tretyakova, Kinetics of O^6-methyl-2′-deoxyguanosine repair by O^6-alkylguanine DNA alkyltransferase within K-ras gene-derived DNA sequences, Chem. Res. Toxicol. 19 (2006) 531–538.
[5] Z.A. Ronai, S. Gradia, L.A. Peterson, S.S. Hecht, G to A transitions and G to T transversions in codon 12 of the Ki-ras oncogene isolated from mouse lung tumors induced by 4-(methylnitrosamino)-1-(3-pyridyl)-1-butanone (NNK) and related DNA methylating and pyridyloxobutylating agents, Carcinogenesis 14 (1993) 2419–2422.
[6] G.C.W.E.C. Friedberg, W. Siede, R.D. Wood, R.A. Schultz, T. Ellenberger, DNA Repair and Mutagenesis, 2nd ed., ASM Press, Washington, DC, 2006, pp. 1–1118.
[7] H.P. Leenhouts, M.J. Brugmans, Calculation of the 1995 lung cancer incidence in The Netherlands and Sweden caused by smoking and radon: risk implications for radon, Radiat. Environ. Biophys. 40 (2001) 11–21.
[8] J.H. Lubin, K. Steindorf, Cigarette use and the estimation of lung cancer attributable to radon in the United States, Radiat. Res. 141 (1995) 79–85.
[9] M. Ikeda, K. Masumura, Y. Sakamoto, B. Wang, M. Nenoi, K. Sakuma, I. Hayata, T. Nohmi, Combined genotoxic effects of radiation and a tobacco-specific nitrosamine in the lung of gpt delta transgenic mice, Mutat. Res. 626 (2007) 15–25.
[10] K. Yamauchi, S. Kakinuma, S. Sudo, S. Kito, Y. Ohta, T. Nohmi, K. Masumura, M. Nishimura, Y. Shimada, Differential effects of low- and high-dose X-rays on N-ethyl-N-nitrosourea-induced mutagenesis in thymocytes of B6C3F1 gpt-delta mice, Mutat. Res. 640 (2008) 27–37.
[11] V.S. Goldmacher, R.A. Cuzick Jr., W.G. Thilly, Isolation and partial characterization of human cell mutants differing in sensitivity to killing and mutation by methylnitrosourea and N-methyl-N′-nitro-N-nitrosoguanidine, J. Biol. Chem. 261 (1986) 12462–12471.
[12] M. Szadkowski, I. Iaccarino, K. Heinimann, G. Marra, J. Jiricny, Characterization of the mismatch repair defect in the human lymphoblastoid MT1 cells, Cancer Res. 65 (2005) 4525–4529.
[13] M. Honma, M. Hayashi, T. Sofuni, Cytotoxic and mutagenic responses to X-rays and chemical mutagens in normal and p53-mutated human lymphoblastoid cells, Mutat. Res. 374 (1997) 89–98.
[14] M. Honma, L.S. Zhang, M. Hayashi, K. Takeshita, Y. Nakagawa, N. Tanaka, T. Sofuni, Illegitimate recombination leading to allelic loss and unbalanced translocation in p53-mutated human lymphoblastoid cells, Mol. Cell. Biol. 17 (1997) 4774–4781.
[15] L. Zhan, H. Sakamoto, M. Sakuraba, D.S. Wu, L.S. Zhang, T. Suzuki, M. Hayashi, M. Honma, Genotoxicity of microcystin-LR in human lymphoblastoid TK6 cells, Mutat. Res. 557 (2004) 1–6.
[16] L.S. Zhang, M. Honma, M. Hayashi, T. Suzuki, A. Matsuoka, T. Sofuni, A comparative study of TK6 human lymphoblastoid and L5178Y mouse lymphoma cell lines in the in vitro micronucleus test, Mutat. Res. 347 (1995) 105–115.
[17] S. Sagar, I.R. Green, Pro-apoptotic activities of novel synthetic quinones in human cancer cell lines, Cancer Lett. 285 (2009) 23–27.
[18] P. Cejka, L. Stojic, N. Mojas, A.M. Russell, K. Heinimann, E. Cannavo, M. di Pietro, G. Marra, J. Jiricny, Methylation-induced G(2)/M arrest requires a full complement of the mismatch repair protein hMLH1, EMBO J. 22 (2003) 2245–2254.
[19] H. Oka, K. Ikeda, H. Yoshimura, A. Ohuchida, M. Honma, Relationship between p53 status and 5-fluorouracil sensitivity in 3 cell lines, Mutat. Res. 606 (2006) 52–60.
[20] A. Yamamoto, T. Nunoshiba, K. Umezu, T. Enomoto, K. Yamamoto, Phenyl hydroquinone, an Ames test-negative carcinogen, induces Hog1-dependent stress response signaling, FEBS J. 275 (2008) 5733–5744.

[21] M.J. Hickman, L.D. Samson, Role of DNA mismatch repair and p53 in signaling induction of apoptosis by alkylating agents, Proc. Natl. Acad. Sci. U.S.A. 96 (1999) 10764–10769.
[22] M. Honma, Generation of loss of heterozygosity and its dependency on p53 status in human lymphoblastoid cells, Environ. Mol. Mutagen. 45 (2005) 162–176.
[23] P. Vernole, B. Tedeschi, L. Tentori, L. Levati, G. Argentin, R. Cicchetti, O. Forini, G. Graziani, S. D'Atri, Role of the mismatch repair system and p53 in the clastogenicity and cytotoxicity induced by bleomycin, Mutat. Res. 594 (2006) 63–77.
[24] F. Bunz, A. Dutriaux, C. Lengauer, T. Waldman, S. Zhou, J.P. Brown, J.M. Sedivy, K.W. Kinzler, B. Vogelstein, Requirement for p53 and p21 to sustain G2 arrest after DNA damage, Science 282 (1998) 1497–1501.
[25] D.R. Duckett, S.M. Bronstein, Y. Taya, P. Modrich, hMutSalpha- and hMutLalpha-dependent phosphorylation of p53 in response to DNA methylator damage, Proc. Natl. Acad. Sci. U.S.A. 96 (1999) 12384–12388.
[26] K. Hafer, K.S. Iwamoto, Z. Scuric, R.H. Schiestl, Adaptive response to gamma radiation in mammalian cells proficient and deficient in components of nucleotide excision repair, Radiat. Res. 168 (2007) 168–174.
[27] T. Ikushima, H. Aritomi, J. Morisita, Radioadaptive response: efficient repair of radiation-induced DNA damage in adapted cells, Mutat. Res. 358 (1996) 193–198.
[28] M.S. Sasaki, Y. Ejima, A. Tachibana, T. Yamada, K. Ishizaki, T. Shimizu, T. Nomura, DNA damage response pathway in radioadaptive response, Mutat. Res. 504 (2002) 101–118.
[29] J.D. Shadley, V. Afzal, S. Wolff, Characterization of the adaptive response to ionizing radiation induced by low doses of X rays to human lymphocytes, Radiat. Res. 111 (1987) 511–517.
[30] J.K. Wiencke, V. Afzal, G. Olivieri, S. Wolff, Evidence that the [^{3}H] thymidine-induced adaptive response of human lymphocytes to subsequent doses of X-rays involves the induction of a chromosomal repair mechanism, Mutagenesis 1 (1986) 375–380.
[31] S. Tapio, V. Jacob, Radioadaptive response revisited, Radiat. Environ. Biophys. 46 (2007) 1–12.
[32] H. Offer, N. Erez, I. Zurer, X. Tang, M. Milyavsky, N. Goldfinger, V. Rotter, The onset of p53-dependent DNA repair or apoptosis is determined by the level of accumulated damaged DNA, Carcinogenesis 23 (2002) 1025–1032.
[33] J.M. Carethers, M.T. Hawn, D.P. Chauhan, M.C. Luce, G. Marra, M. Koi, C.R. Boland, Competency in mismatch repair prohibits clonal expansion of cancer cells treated with N-methyl-N′-nitro-N-nitrosoguanidine, J. Clin. Invest. 98 (1996) 199–206.
[34] M. di Pietro, G. Marra, P. Cejka, L. Stojic, M. Menigatti, M.S. Cattaruzza, J. Jiricny, Mismatch repair-dependent transcriptome changes in human cells treated with the methylating agent N-methyl-N′-nitro-N-nitrosoguanidine, Cancer Res. 63 (2003) 8158–8166.
[35] B. Kaina, M. Christmann, S. Naumann, W.P. Roos, MGMT: key node in the battle against genotoxicity carcinogenicity and apoptosis induced by alkylating agents, DNA Repair (Amst) 6 (2007) 1079–1099.
[36] A.W. Adamson, D.I. Beardsley, W.J. Kim, Y. Gao, R. Baskaran, K.D. Brown, Methylator-induced, mismatch repair-dependent G2 arrest is activated through Chk1 and Chk2, Mol. Biol. Cell 16 (2005) 1513–1526.
[37] S. Caporali, S. Falcinelli, G. Starace, M.T. Russo, E. Bonmassar, J. Jiricny, S. D'Atri, DNA damage induced by temozolomide signals to both ATM and ATR: role of the mismatch repair system, Mol. Pharmacol. 66 (2004) 478–491.
[38] Y. Luo, F.T. Lin, W.C. Lin, ATM-mediated stabilization of hMutL DNA mismatch repair proteins augments p53 activation during DNA damage, Mol. Cell. Biol. 24 (2004) 6430–6444.
[39] Y. Hirose, M. Katayama, D. Stokoe, D.A. Haas-Kogan, M.S. Berger, R.O. Pieper, The p38 mitogen-activated protein kinase pathway links the DNA mismatch repair system to the G2 checkpoint and to resistance to chemotherapeutic DNA-methylating agents, Mol. Cell. Biol. 23 (2003) 8306–8315.
[40] S. Quiros, W.P. Roos, B. Kaina, Processing of O^6-methylguanine into DNA double-strand breaks requires two rounds of replication whereas apoptosis is also induced in subsequent cell cycles, Cell Cycle 9 (2010) 168–178.
[41] W.P. Roos, B. Kaina, DNA damage-induced cell death by apoptosis, Trends Mol. Med. 12 (2006) 440–450.
[42] L.S. Li, J.C. Morales, A. Hwang, M.W. Wagner, D.A. Boothman, DNA mismatch repair-dependent activation of c-Abl/p73alpha/GADD45alpha-mediated apoptosis, J. Biol. Chem. 283 (2008) 21394–21403.

Mutagenesis vol. 26 no. 4 pp. 545–549, 2011
Advance Access Publication 25 March 2011
doi:10.1093/mutage/ger014

Acrylamide genotoxicity in young versus adult *gpt* delta male rats

Naoki Koyama[1,2,3], Manabu Yasui[1], Aoi Kimura[1,4], Shigeaki Takami[5,6], Takuya Suzuki[7], Kenichi Masumura[1], Takehiko Nohmi[1], Shuichi Masuda[2], Naohide Kinae[2], Tomonari Matsuda[7], Toshio Imai[5,8] and Masamitsu Honma[1,*]

[1]Division of Genetics and Mutagenesis, National Institute of Health Sciences, 1-18-1 Kamiyoga, Setagaya-ku, Tokyo 158-8501, Japan, [2]Laboratory of Food Hygiene, School of Food and Nutritional Sciences, University of Shizuoka, 52-1 Yada, Shizuaka-ku, Shizuoka 422-8526, Japan, [3]Drug Safety, Eisai Product Creation Systems, Eisai Co., Ltd, Tokodai 5-1-3 Tsukuba-shi Ibaraki 300-2635, Japan, [4]Drug Safety Research Laboratories, Shin Nippon Biomedical Laboratories, Ltd, Kagoshima 891-1394, Japan, [5]Division of Pathology, National Institute of Health Sciences, 1-18-1 Kamiyoga, Setagaya-ku, Tokyo 158-8501, Japan, [6]Pathology & Clinical Examination Laboratory, Safety Assessment Unit, Biosafety Research Center, Foods, Drugs and Pesticides, 582-2 Shioshinden, Iwata, Shizuoka 437-1213, Japan, [7]Research Center for Environmental Quality Management, Kyoto University, 1-2 Yumihama, Otsu, Shiga, 520-0811, Japan and [8]Central Animal Division, National Cancer Center Research Institute, 1-1 Tsukiji 5-chome, Chuo-ku, Tokyo 104-0045, Japan.

*To whom correspondence should be addressed. Division of Genetics and Mutagenesis, National Institute of Health Sciences, 1-18-1 Kamiyoga, Setagaya-ku, Tokyo 158-8501, Japan. Tel: +81 3 3700 1141 ext. 435; Fax: +81 3 3700 2348; Email: honma@nihs.go.jp

Received on January 28, 2011; revised on February 23, 2011; accepted on February 28, 2011

The recent discovery that the potent carcinogen acrylamide (AA) is present in a variety of fried and baked foods raises health concerns, particularly for children, because AA is relatively high in child-favoured foods such as potato chips and French fries. To compare the susceptibility to AA-induced genotoxicity of young versus adult animals, we treated 3- and 11-week-old male gpt delta transgenic F344 rats with 0, 20, 40 or 80 p.p.m. AA via drinking water for 4 weeks and then examined genotoxicity in the bone marrow, liver and testis. We also analysed the level of *N*7-(2-carbamoyl-2-hydroxyethyl)-guanine (*N*7-GA-Gua), the major DNA adduct induced by AA, in the liver, testis and mammary gland. At 40 and 80 p.p.m., both age groups yield similar results in the comet assay in liver; but at 80 p.p.m., the bone marrow micronucleus frequency and the *gpt*-mutant frequency in testis increased significantly only in the young rats, and *N*7-GA-Gua adducts in the testis was significantly higher in the young rats. These results imply that young rats are more susceptible than adult rats to AA-induced testicular genotoxicity.

Introduction

Acrylamide (AA) is a low molecular weight vinyl compound commonly used in industries and laboratories. Because individuals are exposed to AA in the workplace, health concerns originally centred on occupational exposure (1). A recent study, however, reported that low levels of AA are formed in many heat-processed foods, especially starchy ones such as potato chips, crackers and French fries (2,3), as a result of asparagine reacting with sugars (Maillard reaction) (4,5). This finding raises concerns that AA poses health risks for the general population (6).

Many animal studies have demonstrated that AA induces neurotoxicity, testicular toxicity and reproductive toxicity (7–9). AA also causes cancers such as mammary fibroadenomas, thyroid follicular cell adenomas and testicular mesotheliomas in rats (10–12). In mice, it induces gene mutations in liver, micronuclei in haematopoietic cells (13,14) and chromosome aberrations in spermatids and spermatocytes (15,16). Thus, AA is clearly genotoxic *in vivo*, although its *in vitro* genotoxicity remains unclear because it is not metabolically activated in standard *in vitro* systems (17,18). AA is metabolised to glycidamide (GA), presumably by cytochrome P450 2E1 (CYP2E1), which quickly reacts with cellular DNA and protein (6,19,20). Two major GA–DNA adducts—*N*7-(2-carbamoyl-2-hydroxyethyl)-guanine (*N*7-GA-Gua) and *N*3-(2-carbamoyl-2-hydroxyethyl)-adenine (*N*3-GA-Ade)—have been identified in mice and rats treated with AA or GA (21–23), with the level of *N*7-GA-Gua being 100 times as high as the level of *N*3-GA-Ade in the organs (22). Individual GA to AA ratios, which can be used as an indicator of the extent of AA metabolism, are highly variable, suggesting that some individuals or populations may be more susceptible than others to AA-induced genotoxicity (24). Other issues are AA intake and metabolism in children compared with adults. Children generally consume larger amounts of food relative to their body mass than adults and favour foods such as French fries and potato chips that have relatively high AA concentrations (25). These issues should be considered when evaluating the susceptibility of the paediatric population in genotoxic and carcinogenic risk assessments (26).

In the present study, to compare the susceptibility to AA-induced genotoxicity of young versus, adult age groups, we treated 3- and 11-week-old male *gpt* delta transgenic F344 rats with 0, 20, 40 or 80 p.p.m. of AA via drinking water for 4 weeks and examined genotoxicity in the bone marrow, liver and testis. We also analysed the level of *N*7-GA-Gua in the liver, testis and mammary gland.

Materials and methods

Animals, diet and housing

We purchased 20 male with 10-week-old and 15 pregnant female F344 *gpt* delta transgenic rats from Japan SLC (Shizuoka, Japan). The pregnant animals were time-mated at 10 weeks of age and arrived on gestational Day 12 or 13 to our facility. After delivery, we obtained >14 male pups from the pregnant rats. All animals were housed *three* to *five* rats in polycarbonate cage with sterilised wood chip bedding and maintained under specific pathogen-free standard laboratory conditions: room temperature, 24 ± 1°C; relative humidity, 55 ± 5%; 12-h light–dark cycle; basal diet (CRF-1; Oriental Yeast Company, Tokyo, Japan) and tap water *ad libitum* until parturition.

Treatments of animals

The protocol for this study was approved by the Animal Care and Utilisation Committee of the National Institute of Health Sciences. We randomly divided 14 and 20 of the 3- and 11-week-old rats into four groups of 3–5 animals, treated them for 4 weeks with AA (Wako Pure Chemical Co., Tokyo, Japan) at 0, 20, 40 or 80 p.p.m. in drinking water and monitored clinical signs, body weight and food and water consumption. At the end of the treatment period, we anaesthetized and killed the animals, and we excised organs for the *gpt* mutation assay (liver, testis), comet assay (liver), DNA adducts analysis (liver, testis, mammary gland and thyroid) and micronucleus (MN) test (bone marrow).

MN test

We removed bone marrow from the femur, mixed it with foetal calf serum, placed it on an acridine orange-coated glass slide, covered it with a coverslip and stained it supravitally (27). We analysed 2000 polychromatic erythrocytes per animal with a fluorescence microscope and recorded the number of micronucleated polychromatic erythrocytes, which fluoresced greenish yellow.

Alkaline comet assay

We performed the comet assay using the procedure recommended by the comet assay working group of the International Workshop on Genotoxicity Testing (IWGT) (28,29), except that we used a MAS-coat type slide glass (Matsunami Glass *Ind.* Ltd, Tokyo, Japan) instead of a conventional agarose bottom layer (30). We prepared cell suspensions from the livers, mixed them with 0.5% w/v low-melting agarose, and spotted an aliquot of the mixture onto the slide. After electrophoresis, we stained the cells with SYBR-Gold (cat. # S-11494; Molecular Probes, Invitrogen, Tokyo, Japan), and examined at least 100 cells per animal using a fluorescence microscope (BX50 and BX51; Olympus Corporation, Tokyo, Japan) connected to the comet assay scoring system (Comet IV; Perceptive Instruments Ltd, Suffolk, UK), which quantified the result as %tail intensity.

gpt mutation assay

We extracted high molecular weight genomic DNA from the liver and testis using a Recover Ease DNA Isolation Kit (Stratagene, La Jolla, CA, USA), rescued lambda EG10 phages using Transpack Packaging Extract (Stratagene) and conducted the *gpt* mutation assay as previously published (31). We calculated the *gpt*-mutant frequency (*gpt*-MF) by dividing the number of 6-thioguanine-resistant colonies by the number of colonies with rescued plasmids.

DNA adduct assay

As a standard for liquid chromatography tandem mass spectrometry analysis, *N*7-GA-Gua and [$^{15}N_5$]-labelled *N*7-GA-Gua were synthesised as described previously (18,22). We extracted DNA from the liver, testis, mammary gland and thyroid using a DNeasy 96 Blood & Tissue Kit (QIAGEN, Düsseldorf, Germany), incubated it at 37°C for 48 h for deprination. We added an aliquot of the labelled standard to each sample and filtered through an ultrafiltration membrane to remove DNA. The eluted solution was evaporated thoroughly and dissolved in water and then the solutions were subsequently quantified by a Quattro Ultima Pt triple stage quadrupole mass spectrometer (Waters-Micromass, Milford, MA, USA) equipped with a Shimadzu LC system (Shimadzu, Japan). We analysed the liver and testis for each individual rat but pooled the mammary and thyroid glands for each treatment group because the tissue yields were too small to be examined individually.

Statistical analysis

We used the Student's *t*-test to determine the statistical significance of the difference in the results of the *gpt* mutation assay and the DNA adduct assay between the treated and negative control groups and between the young and adult groups. We examined variances in body weight and results of the MN and comet assays by one-way analysis of variance using the Dunnett's test to compare the differences between the control and treated groups.

Results

Clinical signs, body weight and AA intake

We observed no clinical abnormality in either the young or adult rats during the 28-day treatment period. We found no significant differences in body weight or food and water consumption between the adult treatment groups, although we did observe a slight but statistically insignificant suppression of body weight in the young, 80-p.p.m. treatment group (Table I).

The table shows average daily food, water and AA intake of the young and adult treatment groups and their mean body weights. The average daily intakes of AA are calculated as 3.01, 5.95 and 12.19 mg/kg body weight for 20, 40 and 80 p.p.m. group, respectively, in young rats and as 1.83, 3.54 and 7.05 mg/kg body weight for 20, 40 and 80 p.p.m. group, respectively, in adult rats.

MN test

While no AA dose induced MN in adult rat bone marrow, the highest dose (80 p.p.m.) significantly increased the MN frequency in young rat bone marrow (Figure 1a). Because of the large standard deviation, however, the difference between young and adult rats was not significant (Figure 1a).

Alkaline comet assay

DNA damage induced by AA in liver was evaluated by the comet assay under alkaline conditions (Figure 1b). The comet tail intensities increased in a dose-dependent manner in both young and adult rats with no statistically significant differences between the two groups. AA significantly induced DNA damage at 40 and 80 p.p.m. in the adult rat liver and at 80 p.p.m. in the young rat liver.

gpt mutation assay

Figure 2 shows the *gpt* mutation assay results. The *gpt*-MF of control (0 p.p.m.) young and adult rat livers was 1.57 ± 0.72 ($\times 10^{-6}$) and 3.66 ± 2.14 ($\times 10^{-6}$), respectively. The control *gpt*-MF of the young rat liver was lower than that of the adult rat liver, but not significantly. AA did not increase the *gpt*-MF in the liver of either age group at any dose; but at 80 p.p.m., it approximately doubled the *gpt*-MF in the testis of both young and adult rats, but the increase in adult rats was not statistically significant.

DNA adduct formation

Figure 3 shows *N*7-GA-Gua DNA adduct levels in the liver, testis and mammary glands and thyroid of the young and adult rats. The adduct level increased in a dose-dependent manner in all the tissues. In the mammary glands and thyroid, adduct levels did not differ significantly between young and adult rats. In the liver and testis, on the other hand, the level was higher in the young rats than in the adult rats. In the testis, the DNA adduct level of young rats was approximately six times that of adult rats at all treatment doses.

Discussion

The *in vivo* genotoxicity of AA has been clearly demonstrated by various rodent genotoxicity tests including MN tests in peripheral blood (13,14,32) and gene mutation and comet assays in various organs (14,33,34). However, there has been no report for the comparison of genotoxicity between young and adult animals. In this study of the genotoxicity of AA in various organs of young (3-week-old) and adult (11-week-old) male rats, we showed that the testis were more vulnerable to AA genotoxicity in the young rat than in the adult rat. Especially, *N*7-GA-Gua DNA adduct was much higher accumulated in the testis of young rats than of adult rats (Figure 3). The daily intake of AA per weight in young rats was ~1.5-fold of the adult rats because the younger animals drank more water. It can explain the higher accumulation of adduct in the young rat liver, but the level in testis was

Table I. Body weight, food and water consumption and AA intake of young and adult rats

Group	AA dose (p.p.m.)	No. of animals	Initial body weight (g) mean ± SD	Final body weight (g) mean ± SD	Food consumption (mg/rat/day)	Water consumption (ml/rat/day)	Intake of AA (mg/kg/day)
Young	0	4	40.5 ± 2.7	168.9 ± 14.3	11.2	17.9	0
	20	3	37.1 ± 3.5	164.7 ± 17.8	11.3	16.9	3.01
	40	3	38.2 ± 2.1	165.1 ± 3.6	11.1	16.7	5.95
	80	4	40.6 ± 2.5	157.4 ± 8.2	11.0	16.9	12.19
Adult	0	5	249.8 ± 10.0	301.3 ± 11.5	16.4	25.8	0
	20	5	249.8 ± 8.2	299.9 ± 7.3	16.1	25.4	1.83
	40	5	250.5 ± 8.7	302.4 ± 12.2	16.2	24.8	3.54
	80	5	249.1 ± 7.7	306.6 ± 5.4	16.8	24.6	7.05

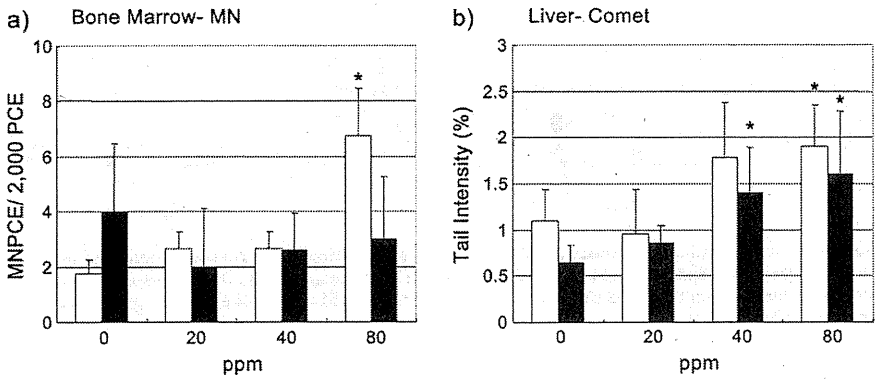

Fig. 1. (**a**) MN frequency in bone marrow of AA-treated young (open bars) and adult (closed bars) *gpt* delta rats. (**b**) Tail intensity (%) in the comet assay in liver of AA-treated young (open bars) and adult (closed bars) *gpt* delta rats. The values represent the mean of experiments ± standard deviations. *is statistically significant experiment compared with the untreated control ($P < 0.05$)discussion.

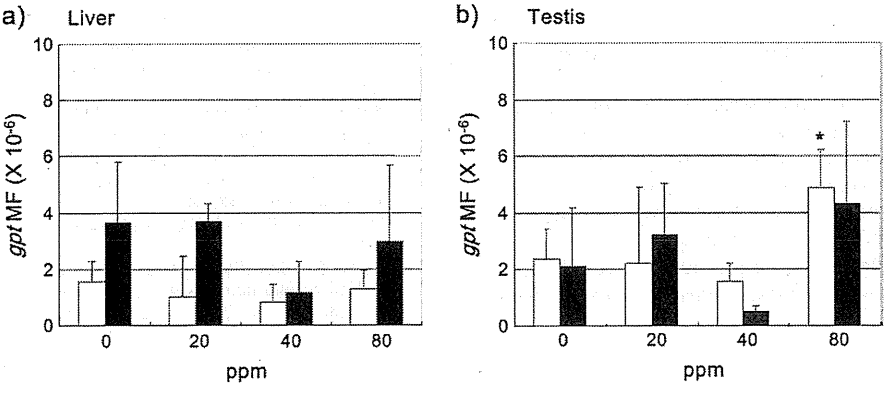

Fig. 2. *gpt* Mutation frequency in liver (**a**) and testis (**b**) of AA administered young (open bars) and adult (closed bars) *gpt* delta rats. The values represent the mean of experiments ± standard deviations. *is statistically significant experiment compared with the untreated control ($P < 0.05$).

approximately six times high in the young rats than in the adult rats, suggesting that AA metabolism in testis is different depending on animal age. Testis is one of the target organs of AA-induced genotoxicity (15,16,35–39). We believe that this is the first report of an age difference in the effect.

AA is primarily metabolised in animals via two competing pathways: oxidation by CYP2E1 to form GA (activation) and conjugation by glutathione *S*-transferase (GST) with reduced glutathione (detoxification) (19,40,41). GA may subsequently undergo conjugation or hydrolysis catalysed by epoxide hydrolase. The balance between activation and detoxification probably determines AA genotoxicity *in vivo*. Rat testis shows CYP2E1 activity (42). Wang *et al.* (43) reported that the treatment of 1.4 and 7.0 mM of AA or GA via drinking water for 4 weeks induced the testicular *cII* mutation in Big Blue mice. The *cII* mutation spectra significantly differed between testis and liver, suggesting that testis may have different pathway to metabolise AA and GA. However, the

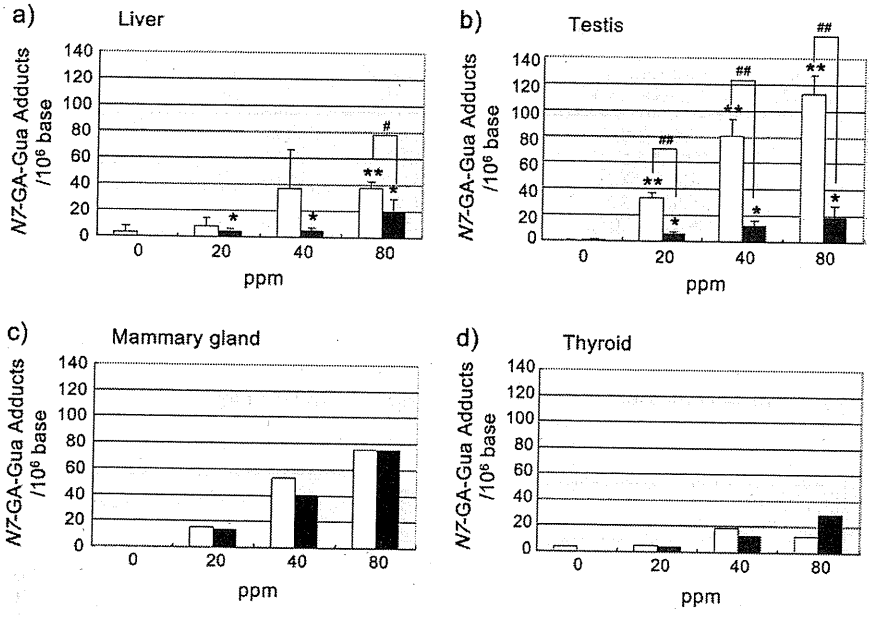

Fig. 3. Levels of *N*7-GA-Gua in the liver (**a**) testis (**b**) mammary gland (**c**) thyroid and (**d**) administered AA young (open bars) and adult (closed bars) *gpt* delta rat. The mammary gland and thyroid were pooled and analysed in the treatment group. Data are expressed as the number of adducts in 10^6 nucleotides. * and **are statistically significant experiment compared with the untreated control ($*P < 0.05$, $**P < 0.05$). # and ##are statistically significant experiment compared between young and adult *gpt* delta rat ($\#P < 0.05$, $\#\#P < 0.05$).

developmental changes were not studied. Recently, Takahashi *et al.*. (44) showed that GST activity in the testis was significantly lower in young rats than in adult rats and that could explain the different age-related *N*7-GA-Gua adduct levels and *gpt*-MFs in the present study. The greater mutagenicity of aflatoxin B1 in liver of neonatal mice than of adult mice corresponds to liver GST levels (45). The GST level in the organs could be responsible for the expression of genotoxicity of AA and aflatoxin B1.

While the *N*7-GA-Gua adduct level in liver and testis clearly increased in a dose-dependent manner and significantly differed between young and adult rats, the *gpt* mutation results were not clear. We treated the rats with doses that were lower than those used in other studies (14,34,43), and these doses may have been insufficient to induce gene mutations in our study. Indication of the DNA adduct must be good biomarker to demonstrate genotoxic insult under low-dose exposure condition.

In conclusion, this finding that young rats were more susceptible than adult rats to AA-induced genotoxicity, especially in the testis, suggests that we should be concerned about the risk to children exposed to AA via ordinary foods.

Funding

Health, Labour and Wealth Science Research Grant in Japan (H21-food-general-012), Human Science Foundation in Japan (KHB1006).

Acknowledgements

The authors are grateful to Dr Miriam Bloom (SciWrite Biomedical Writing & Editing Services) for providing professional editing.

Conflict of interest statement: None declared.

References

1. Bergmark, E. (1997) Hemoglobin adducts of acrylamide and acrylonitrile in laboratory workers, smokers and nonsmokers. *Chem. Res. Toxicol.*, **10**, 78–84.
2. Tareke, E., Rydberg, P., Karlsson, P., Eriksson, S. and Tornqvist, M. (2002) Analysis of acrylamide, a carcinogen formed in heated foodstuffs. *J. Agric. Food Chem.*, **50**, 4998–5006.
3. Tareke, E., Rydberg, P., Karlsson, P., Eriksson, S. and Tornqvist, M. (2000) Acrylamide: a cooking carcinogen? *Chem. Res. Toxicol.*, **13**, 517–522.
4. Mottram, D. S., Wedzicha, B. L. and Dodson, A. T. (2002) Acrylamide is formed in the Maillard reaction. *Nature*, **419**, 448–449.
5. Stadler, R. H., Blank, I., Varga, N., Robert, F., Hau, J., Guy, P. A., Robert, M. C. and Riediker, S. (2002) Acrylamide from Maillard reaction products. *Nature*, **419**, 449–450.
6. Rice, J. M. (2005) The carcinogenicity of acrylamide. *Mutat. Res.*, **580**, 3–20.
7. Tyl, R. W., Marr, M. C., Myers, C. B., Ross, W. P. and Friedman, M. A. (2000) Relationship between acrylamide reproductive and neurotoxicity in male rats. *Reprod. Toxicol.*, **14**, 147–157.
8. Yang, H. J., Lee, S. H., Jin, Y., Choi, J. H., Han, C. H. and Lee, M. H. (2005) Genotoxicity and toxicological effects of acrylamide on reproductive system in male rats. *J. Vet. Sci.*, **6**, 103–109.
9. LoPachin, R. M., Balaban, C. D. and Ross, J. F. (2003) Acrylamide axonopathy revisited. *Toxicol. Appl. Pharmacol.*, **188**, 135–153.
10. Carere, A. (2006) Genotoxicity and carcinogenicity of acrylamide: a critical review. *Ann. Ist. Super. Sanita*, **42**, 144–155.
11. Besaratinia, A. and Pfeifer, G. P. (2007) A review of mechanisms of acrylamide carcinogenicity. *Carcinogenesis*, **28**, 519–528.
12. IARC (1994) Acrylamide. In: IARC Monographs on the Evaluation of Carcinogen Risk to Human: Some Industrial Chemicals. International Agency for Research on Cancer Lyon, France, 60, pp. 389–433.
13. Abramsson-Zetterberg, L. (2003) The dose-response relationship at very low doses of acrylamide is linear in the flow cytometer-based mouse micronucleus assay. *Mutat. Res.*, **535**, 215–222.
14. Manjanatha, M. G., Aidoo, A., Shelton, S. D., Bishop, M. E., MacDaniel, L. P., Lyn-Cock, L. E. and Doerge, D. R. (2006) Genotoxicity of acrylamide and its metabolite glycidamide administrated in drinking water to male and female Big Blue mice. *Environ. Mol. Mutagen.*, **47**, 6–17.

15. Dearfield, K. L., Douglas, G. R., Ehling, U. H., Moore, M. M., Sega, G. A. and Brusick, D. J. (1995) Acrylamide: a review of its genotoxicity and an assessment of heritable genetic risk. *Mutat. Res.*, **330**, 71–99.
16. Dearfield, K. L., Abernathy, C. O., Ottley, M. S., Brantner, J. H. and Hayes, P. F. (1988) Acrylamide: its metabolism, developmental and reproductive effects, genotoxicity, and carcinogenicity. *Mutat. Res.*, **195**, 45–77.
17. Koyama, N., Sakamoto, H., Sakuraba, M. *et al.* (2006) Genotoxicity of acrylamide and glycidamide in human lymphoblastoid TK6 cells. *Mutat. Res.*, **603**, 151–158.
18. Koyama, N., Yasui, M., Oda, Y. *et al.* (2011) Genotoxicity of acrylamide in vitro: acrylamide is not metabolically activated in standard in vitro systems. *Environ. Mol. Mutagen.*, **52**, 12–19.
19. Sumner, S. C., Fennell, T. R., Moore, T. A., Chanas, B., Gonzalez, F. and Ghanayem, B. I. (1999) Role of cytochrome P450 2E1 in the metabolism of acrylamide and acrylonitrile in mice. *Chem. Res. Toxicol.*, **12**, 1110–1116.
20. Ghanayem, B. I., McDaniel, L. P., Churchwell, M. I., Twaddle, N. C., Snyder, R., Fennell, T. R. and Doerge, D. R. (2005) Role of CYP2E1 in the epoxidation of acrylamide to glycidamide and formation of DNA and hemoglobin adducts. *Toxicol. Sci.*, **88**, 311–318.
21. Doerge, D. R., Young, J. F., McDaniel, L. P., Twaddle, N. C. and Churchwell, M. I. (2005) Toxicokinetics of acrylamide and glycidamide in B6C3F1 mice. *Toxicol. Appl. Pharmacol.*, **202**, 258–267.
22. Gamboa, d. C., Churchwell, M. I., Hamilton, L. P., Von Tungeln, L. S., Beland, F. A., Marques, M. M. and Doerge, D. R. (2003) DNA adduct formation from acrylamide via conversion to glycidamide in adult and neonatal mice. *Chem. Res. Toxicol.*, **16**, 1328–1337.
23. Segerback, D., Calleman, C. J., Schroeder, J. L., Costa, L. G. and Faustman, E. M. (1995) Formation of N-7-(2-carbamoyl-2-hydroxyethyl)guanine in DNA of the mouse and the rat following intraperitoneal administration of [14C]acrylamide. *Carcinogenesis*, **16**, 1161–1165.
24. Neafsey, P., Ginsberg, G., Hattis, D., Johns, D. O., Guyton, K. Z. and Sonawane, B. (2009) Genetic polymorphism in CYP2E1: population distribution of CYP2E1 activity. *J. Toxicol. Environ. Health B Crit. Rev.*, **12**, 362–388.
25. Mucci, L. A. and Wilson, K. M. (2008) Acrylamide intake through diet and human cancer risk. *J. Agric. Food Chem.*, **56**, 6013–6019.
26. Spivey, A. (2010) A matter of degrees: advancing our understanding of acrylamide. *Environ. Health Perspect.*, **118**, A160–A167.
27. Hayashi, M., Sofuni, T. and Morita, T. (1991) Simulation study of the effects of multiple treatments in the mouse bone marrow micronucleus test. *Mutat. Res.*, **252**, 281–287.
28. Tice, R. R., Agurell, E., Anderson, D. *et al.* (2000) Single cell gel/comet assay: guidelines for in vitro and in vivo genetic toxicology testing. *Environ. Mol. Mutagen.*, **35**, 206–221.
29. Burlinson, B., Tice, R. R., Speit, G. *et al.* (2007) Fourth International Workgroup on Genotoxicity testing: results of the in vivo Comet assay workgroup. *Mutat. Res.*, **627**, 31–35.
30. Kimura, A., Torigoe, N., Miyata, A. and Honma, M. (2010) Validation of a simple in vitro comet assay method using CHL cells. *Genes Environ.*, **32**, 61–65.
31. Nohmi, T., Suzuki, T. and Masumura, K. (2000) Recent advances in the protocols of transgenic mouse mutation assays. *Mutat. Res.*, **455**, 191–215.
32. Cao, J., Beisker, W., Nusse, M. and Adler, I. D. (1993) Flow cytometric detection of micronuclei induced by chemicals in poly- and normochromatic erythrocytes of mouse peripheral blood. *Mutagenesis*, **8**, 533–541.
33. Ghanayem, B. I., Witt, K. L., Kissling, G. E., Tice, R. R. and Recio, L. (2005) Absence of acrylamide-induced genotoxicity in CYP2E1-null mice: evidence consistent with a glycidamide-mediated effect. *Mutat. Res.*, **578**, 284–297.
34. Mei, N., McDaniel, L. P., Dobrovolsky, V. N. *et al.* (2010) The genotoxicity of acrylamide and glycidamide in big blue rats. *Toxicol. Sci.*, **115**, 412–421.
35. Takahashi, M., Shibutani, M., Inoue, K., Fujimoto, H., Hirose, M. and Nishikawa, A. (2008) Pathological assessment of the nervous and male reproductive systems of rat offspring exposed maternally to acrylamide during the gestation and lactation periods - a preliminary study. *J. Toxicol. Sci.*, **33**, 11–24.
36. Xiao, Y. and Tates, A. D. (1994) Increased frequencies of micronuclei in early spermatids of rats following exposure of young primary spermatocytes to acrylamide. *Mutat. Res.*, **309**, 245–253.
37. Lahdetie, J., Suutari, A. and Sjoblom, T. (1994) The spermatid micronucleus test with the dissection technique detects the germ cell mutagenicity of acrylamide in rat meiotic cells. *Mutat. Res.*, **309**, 255–262.
38. Shelby, M. D., Cain, K. T., Cornett, C. V. and Generoso, W. M. (1987) Acrylamide: induction of heritable translocation in male mice. *Environ. Mutagen.*, **9**, 363–368.
39. Adler, I. D., Reitmeir, P., Schmoller, R. and Schriever-Schwemmer, G. (1994) Dose response for heritable translocations induced by acrylamide in spermatids of mice. *Mutat. Res.*, **309**, 285–291.
40. Wu, Y. Q., Yu, A. R., Tang, X. Y., Zhang, J. and Cui, T. (1993) Determination of acrylamide metabolite, mercapturic acid by high performance liquid chromatography. *Biomed. Environ. Sci.*, **6**, 273–280.
41. Calleman, C. J., Bergmark, E. and Costa, L. G. (1990) Acrylamide is metabolized to glycidamide in the rat: evidence from hemoglobin adduct formation. *Chem. Res. Toxicol.*, **3**, 406–412.
42. Jiang, Y., Kuo, C. L., Pernecky, S. J. and Piper, W. N. (1998) The detection of cytochrome P450 2E1 and its catalytic activity in rat testis. *Biochem. Biophys. Res. Commun.*, **246**, 578–583.
43. Wang, R. S., McDaniel, L. P., Manjanatha, M. G., Shelton, S. D., Doerge, D. R. and Mei, N. (2010) Mutagenicity of acrylamide and glycidamide in the testes of big blue mice. *Toxicol. Sci.*, **117**, 72–80.
44. Takahashi, M., Inoue, K., Koyama, N., Yoshida, M., Irie, K., Morikawa, T., Shibutani, M., Honma, M. and Nishikawa, A. (2011) Life stage-related differences in susceptibility to acrylamide-induced neural and testicular toxicity. *Arch Toxicol*, (Epub ahead of print).
45. Chen, T., Heflich, R. H., Moore, M. M. and Mei, N. (2010) Differential mutagenicity of aflatoxin B1 in the liver of neonatal and adult mice. *Environ. Mol. Mutagen.*, **51**, 156–163.

doi:10.1016/j.jmb.2011.01.005 J. Mol. Biol. (2011) 406, 679–686

Contents lists available at www.sciencedirect.com

Journal of Molecular Biology

journal homepage: http://ees.elsevier.com.jmb

Mutational Specificities of Brominated DNA Adducts Catalyzed by Human DNA Polymerases

Akira Sassa[1,2], Toshihiro Ohta[2], Takehiko Nohmi[1], Masamitsu Honma[1] and Manabu Yasui[1]*

[1]*Division of Genetics and Mutagenesis, National Institute of Health Sciences, Setagaya-ku, Tokyo 158-8501, Japan*
[2]*School of Life Sciences, Tokyo University of Pharmacy and Life Sciences, Hachiouji-shi, Tokyo 192-0392, Japan*

Received 30 September 2010; received in revised form 24 December 2010; accepted 4 January 2011
Available online 15 January 2011

Edited by J. Karn

Keywords:
inflammation;
hypobromous acid;
halogenation;
translesion synthesis;
mutagenesis

Chronic inflammation is known to lead to an increased risk for the development of cancer. Under inflammatory condition, cellular DNA is damaged by hypobromous acid, which is generated by myeloperoxidase and eosinophil peroxidase. The reactive brominating species induced brominated DNA adducts such as 8-bromo-2′-deoxyguanosine (8-Br-dG), 8-bromo-2′-deoxyadenosine (8-Br-dA), and 5-bromo-2′-deoxycytidine (5-Br-dC). These DNA lesions may be implicated in carcinogenesis. In this study, we analyzed the miscoding properties of the brominated DNA adducts generated by human DNA polymerases (pols). Site-specifically modified oligodeoxynucleotides containing a single 8-Br-dG, 8-Br-dA, or 5-Br-dC were used as a template in primer extension reactions catalyzed by human pols α, κ, and η. When 8-Br-dG-modified template was used, pol α primarily incorporated dCMP, the correct base, opposite the lesion, along with a small amount of one-base deletion (4.8%). Pol κ also promoted one-base deletion (14.2%), accompanied by misincorporation of dGMP (9.5%), dAMP (8.0%), and dTMP (6.1%) opposite the lesion. Pol η, on the other hand, readily bypassed the 8-Br-dG lesion in an error-free manner. As for 8-Br-dA and 5-Br-dC, all the pols bypassed the lesions and no miscoding events were observed. These results indicate that only 8-Br-dG, and not 5-Br-dC and 8-Br-dA, is a mutagenic lesion; the miscoding frequency and specificity vary depending on the DNA pol used. Thus, hypobromous acid-induced 8-Br-dG adduct may increase mutagenic potential at the site of inflammation.

Introduction

Chronic parasitic infections lead to inflammation, and chronic inflammation has been recognized as a factor of carcinogenesis and linked to cancer development.[1] At sites of inflammation, neutrophils and eosinophils are activated and then increased in the blood and tissues.[2] These elements play important roles in host defense against microbial parasite using reactive oxidants such as nitric oxide and hypobromous acid (HOBr).[3] The excessive oxidants in this process, however, can produce several DNA base damages[4–6] and may lead to mutagenesis in adjacent epithelial cells.

*Corresponding author. E-mail address: m-yasui@nihs.go.jp.

Abbreviations used: HOBr, hypobromous acid; MPO, myeloperoxidase; EPO, eosinophil peroxidase; 8-Br-dG, 8-bromo-2′-deoxyguanosine; 8-Br-dA, 8-bromo-2′-deoxyadenosine; 5-Br-dC, 5-bromo-2′-deoxycytidine; 8-Oxo-dG, 8-oxo-7,8-dihydro-2′-deoxyguanosine; dNTP, 2′-deoxynucleoside triphosphate; Alexa546, AlexaFluor-546 dye; pol, human DNA polymerase; F_{ins}, frequency of insertion; F_{ext}, frequency of extension; LPS, lipopolysaccharide; 5-Br-dU, 5-bromo-2′-deoxyuridine.

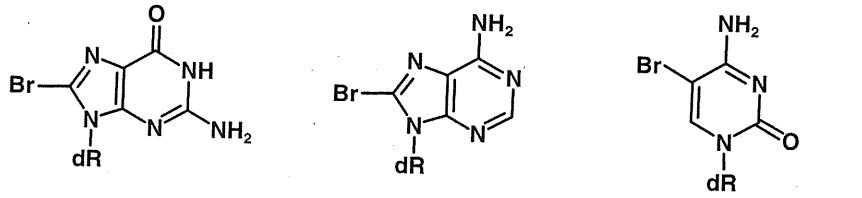

Fig. 1. Structures of brominated DNA adduct.

At the inflammation site, the NADPH oxidase complex of leukocytes is activated and assembles at the plasma membrane. The complex catalyzes the one-electron reduction of oxygen to superoxide (O_2^-). This reduced oxygen then dismutates to hydrogen peroxide (H_2O_2), which is utilized as a reactive oxidant. In the presence of plasma halides (Cl^-, 100 mM; Br^-, 20–100 μM; I^-, <1 μM),[7] myeloperoxidase (MPO) and eosinophil peroxidase (EPO), which are released by neutrophils and eosinophils, respectively, generate HOBr using H_2O_2 and Br^- as substrates (Eq. 1).[3,8–10]

$$Br^- + H_2O_2 + H^+ \rightarrow HOBr + H_2O \quad (1)$$

HOBr is a potent oxidant that oxidizes the cellular components of invading pathogens. This reactive brominating species also damages the host DNA and the cellular protein under chronic inflammatory conditions.[11,12] 5-Bromouracil (5-bromo-2′-deoxyuridine (5-Br-dU) in nucleoside form) has been detected in human inflammatory tissues.[13] 5-Br-dU is well known as a thymidine analog and causes G:C → A:T and A:T → G:C transitions.[14,15] It has been previously reported that 5-bromo-2′-deoxycytidine (5-Br-dC) is produced by EPO and can be converted to 5-Br-dU by cellular cytidine deaminases.[4,16,17] 8-Bromo-2′-deoxyguanosine (8-Br-dG) and 8-bromo-2′-deoxyadenosine (8-Br-dA) are also generated by exposure of calf thymus DNA or free deoxyribonucleoside to the EPO/H_2O_2/Br^- system[6] (Fig. 1). Moreover, 8-Br-dG was recently detected from the hepatic DNA of lipopolysaccharide (LPS)-treated rats and the urine of hepatocellular carcinoma patients.[5] Thus, 5-Br-dC, 8-Br-dA, and 8-Br-dG may contribute to the burden of carcinogenesis in inflammatory tissues.

Primer extension reactions past 8-Br-dG lesion have been performed by using only human DNA polymerase (pol) α and β in the presence of a single or two 2′-deoxynucleoside triphosphates (dNTPs) on single-stranded gap DNA templates containing a 8-Br-dG lesion.[18] The previous report showed that both pols incorporated dCMP and dGMP opposite 8-Br-dG. The miscoding properties of 5-Br-dC and 8-Br-dA have not been determined yet. No quantitative analysis has been used for exploring miscoding events generated by 8-Br-dG, 8-Br-dA, and 5-Br-dC.

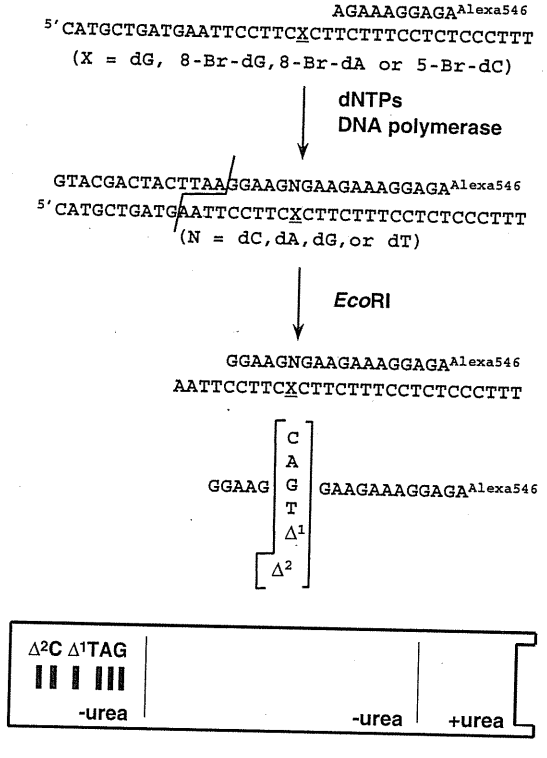

Fig. 2. Diagram of the fluorescent two-phase PAGE analysis. Unmodified and modified 38-mer templates were annealed to an Alexa546-labeled 10-mer primer. Primer extension reactions catalyzed by pols α, κ, and η were conducted in the presence of all four dNTPs. Fully extended products formed during DNA synthesis were recovered from the 20% polyacrylamide gel, annealed with the complementary 38-mer, cleaved with EcoRI, and subjected to two-phase PAGE. To determine miscoding specificities, mobilities of the reaction products were compared with those of 18-mer standards containing dC, dA, dG, or dT opposite the lesion and one-base (Δ^1) or two-base (Δ^2) deletions.

In this study, site-specifically modified oligodeoxynucleotides containing single 8-Br-dG, 8-Br-dA, and 5-Br-dC were used as a DNA template for primer extension reactions catalyzed by human DNA pols α, κ, and η in the presence of all four dNTPs. We determined the miscoding properties of the brominated DNA lesions that occurred during *in vitro* DNA replication using two-phase gel electrophoresis, which allows the quantification of base substitutions and deletions (Fig. 2).[19–21] Relative bypass frequencies past the brominated DNA adducts were also determined by steady-state kinetic studies.

Results

Primer extension reactions catalyzed by human DNA pols on 8-Br-dG-, 8-Br-dA-, and 5-Br-dC-modified DNA templates

Primer extension reactions were carried out using 8-Br-dG-, 8-Br-dA-, and 5-Br-dC-modified 38-mer templates in the presence of all four dNTPs and varying amounts of pol α, κ, or η (Fig. 3). Using the unmodified DNA template, the primer extension rapidly occurred to form fully extended products. When the 5-Br-dC-modified template was used, these pols readily bypassed the lesion, and the bypass efficiency was almost the same as that of the unmodified dC template (Fig. 3). With 8-Br-dG- and 8-Br-dA-modified templates, the primer extension reactions catalyzed by pols α and κ were slightly retarded by the lesions, showing that pols α and κ were blocked opposite (13-mer) and one base before (12-mer) both lesions, respectively (Fig. 3a and b). When the amount of pols was increased, products representing more than 32-mer bases long were produced on the 8-Br-dG- and 8-Br-dA-modified templates. Pol η easily bypassed the 8-Br-dG and 8-Br-dA lesions as efficiently as unmodified dG and dA, respectively (Fig. 3c). Blunt-end addition to the fully extended product (33- to 34-mer) was observed in all primer extension reactions, as reported earlier for *Escherichia coli* and mammalian DNA pols.[22,23]

Miscoding frequencies and specificities of brominated DNA adducts

Translesion synthesis catalyzed by pols α, κ, and η was conducted in the presence of all four dNTPs. The fully extended products (approximately 28- to 34-mer) past 8-Br-dG-, 8-Br-dA-, and 5-Br-dC-modified adducts were recovered, digested by EcoRI, and subjected to two-phase PAGE for quantitative analysis of base substitutions and deletions as described in Materials and Methods. A standard mixture of six Alexa Flour 546 dye (Alexa546)-labeled oligomers containing dC, dA, dG, or dT opposite the lesion or one- and two-base deletions can be resolved by this method (Fig. 2). The percentage of 2′-deoxynucleoside monophosphate incorporation was normalized to the amount of the starting primer.

When unmodified dG template was used, the incorporation of dCMP, the correct base, was observed opposite dG at 74.1%, 85.3%, and 65.7% of the starting primers for pols α, κ, and η, respectively (Fig. 4). Using 8-Br-dG-modified template, pol α frequently incorporated dCMP (69.9%) opposite the lesion. As indicated by the arrowhead in Fig. 4a, one-base deletion (4.8%) was also detected. With pol κ, the correct base dCMP (55.2%) opposite the lesion was incorporated as the primary product. Moreover, pol κ promoted one-base deletion (14.2%) associated with dGMP (9.5%), dAMP (8.0%), and dTMP (6.1%) misincorporation opposite the 8-Br-dG lesion (Fig. 4b). Pol η exclusively incorporated dCMP opposite both unmodified dG and 8-Br-dG (Fig. 4c). Small amounts of unknown products were also detected (arrowheads in Fig. 4c). The miscoding specificities of 8-Br-dA and 5-Br-dC catalyzed by pols α, κ, and η were also determined by using two-phase PAGE. All the pols exclusively incorporated the correct bases dTMP and dGMP opposite 8-Br-dA and 5-Br-dC lesions, respectively, indicating that no miscoding events occurred (Supplementary Fig. S1).

Steady-state kinetic studies on 8-Br-dG-modified DNA template

A steady-state kinetic analysis was performed by using pols α and κ to determine the frequency of dNTP incorporation (F_{ins}) opposite 8-Br-dG and chain extension (F_{ext}) from the primer terminus (Table 1). With pol α, the F_{ins} value for dGTP (0.22), the wrong base, was 2.4 times higher than that for dCTP (9.20×10^{-2}). The relative bypass frequency ($F_{ins} \times F_{ext}$) past dG:8-Br-dG (5.48×10^{-6}) was, however, 13.1 times lower than that for dC:8-Br-dG (7.16×10^{-5}) because the F_{ext} for the dG:8-Br-dG pair (2.49×10^{-5}) was 31.2 times lower than that for the dC:8-Br-dG pair (7.78×10^{-4}). The values of F_{ins} and F_{ext} for dA:8-Br-dG and dT:8-Br-dG were not detectable.

When pol κ was used, the F_{ins} value for dCTP (9.82×10^{-2}) opposite 8-Br-dG was only 1.4 times lower than that for dGTP (0.14) and 13.4 and 15.2 times higher than that for dATP (7.32×10^{-3}) and dTTP (6.46×10^{-3}), respectively. The F_{ext} for dC:8-Br-dG (3.05×10^{-2}) was 12.0, 26.1, and 14.0 times higher than that for dG:8-Br-dG (2.54×10^{-3}), dA:8-Br-dG (1.17×10^{-3}), and dT:8-Br-dG (2.18×10^{-3}), respectively. Therefore, the relative bypass frequency past the dC:8-Br-dG was only 8.43 times higher than that for dG:8-Br-dG.

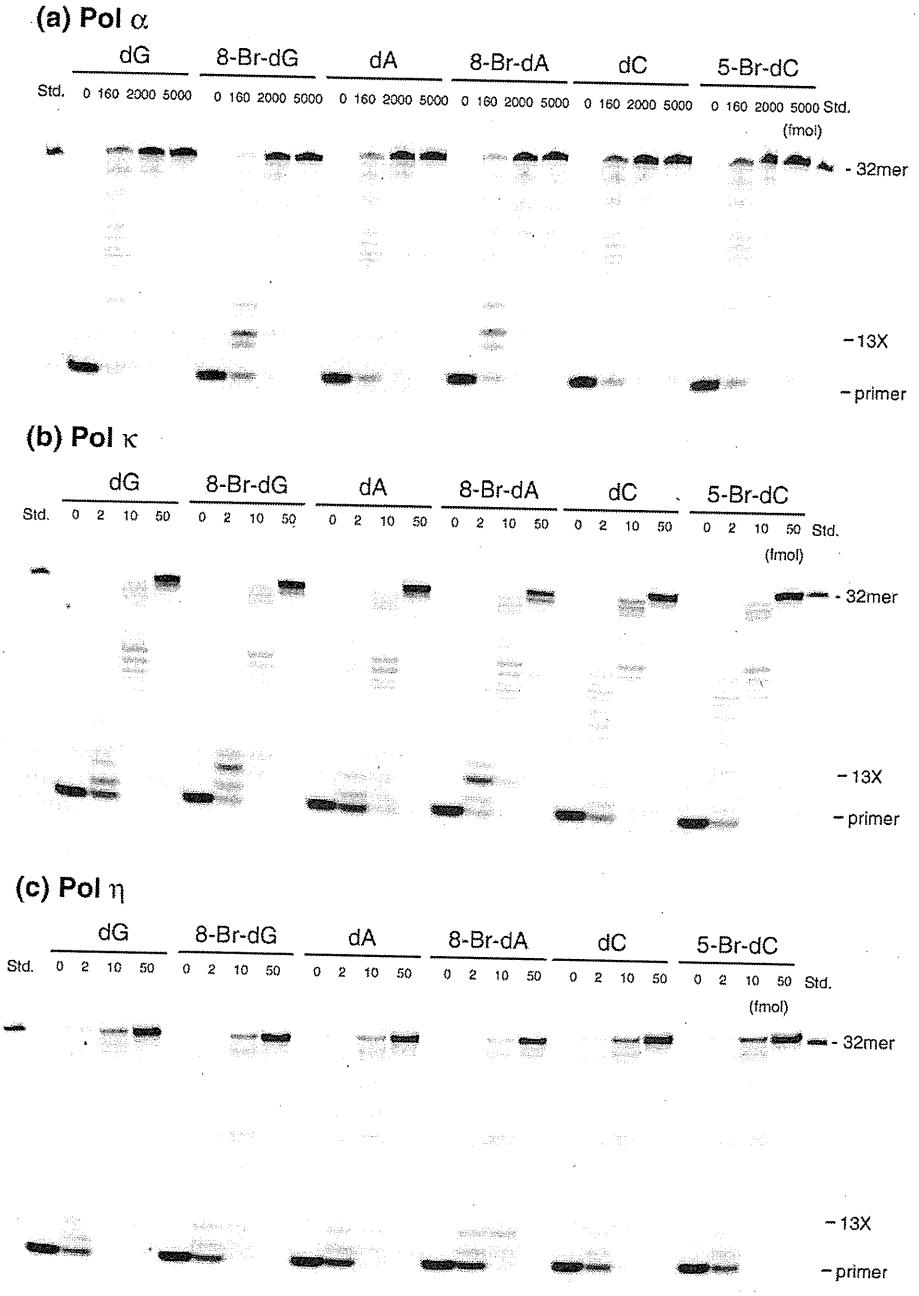

Fig. 3. Primer extension reactions catalyzed by DNA pols on 8-Br-dG-, 8-Br-dA-, and 5-Br-dC-modified DNA templates. Unmodified and modified 38-mer templates were annealed to an Alexa546-labeled 10-mer primer. Primer extension reactions catalyzed by variable amounts (0–5000 fmol) of pols α, κ, and η were conducted at 25 °C for 30 min in the presence of four dNTPs using variable amounts of enzymes. The whole amount of the reaction mixture was subjected to 20% denaturing PAGE. 13X marks the location opposite the DNA adducts.

Discussion

8-Br-dG, 8-Br-dA, and 5-Br-dC can be produced by HOBr *in vitro*,[6,16] and 8-Br-dG has been detected in the genomic DNA of rat liver.[5] If the adducts are not rapidly repaired, DNA pols are more likely to be associated with mutagenic events generated by brominated DNA damage. We demonstrated that primer extension reactions catalyzed by pols α, κ, and η were carried out on site-specifically modified DNA templates containing the 8-Br-dG, 8-Br-dA, or 5-Br-dC lesion. Pols α and κ were slightly retarded

Table 1. Kinetic parameters for nucleotide insertion and chain extension reactions catalyzed by human DNA pols α and κ

		Insertion			Extension			
		dNTP ↓GAAGAAAGGAGA 5′-CCTTCXCTTCTTTCCTCTCCCTTT			dGTP ↓NGAAGAAAGGAGA 5′-CCTTCXCTTCTTTCCTCTCCCTTT			
	N:X	K_m (μM)[a]	V_{max} (% min-1)[a]	F_{ins}	K_m (μM)[a]	V_{max} (% min^{-1})[a]	F_{ext}	$F_{ins} \times F_{ext}$
Pol α	C:G	0.85±0.18	0.053±0.0029	1	1.68±0.31	0.27±0.013	1	1
	C:X	24.4±9.73	0.014±0.0024	9.20×10^{-2}	287.8±68.8	0.036±0.0042	7.78×10^{-4}	7.16×10^{-5}
	A:X	N.D.	N.D.	N.D.	N.D.	N.D.	N.D.	N.D.
	G:X	0.28±0.17	0.00038±0.000017	0.22	400.5±117.7	0.0016±0.00026	2.49×10^{-5}	5.48×10^{-6}
	T:X	N.D.	N.D.	N.D.	N.D.	N.D.	N.D.	N.D.
Pol κ	C:G	5.06±1.76	9.16±1.40	1	0.37±0.08	5.15±0.45	1	1
	C:X	13.0±4.98	2.31±0.31	9.82×10^{-2}	16.1±4.88	6.84±1.09	3.05×10^{-2}	3.00×10^{-3}
	A:X	215±68.0	2.85±0.40	7.32×10^{-3}	149.5±34.3	2.43±0.29	1.17×10^{-3}	8.55×10^{-6}
	G:X	4.02±1.04	1.03±0.08	0.14	90.0±25.5	3.19±0.40	2.54×10^{-3}	3.56×10^{-4}
	T:X	257±66.1	3.01±0.37	6.46×10^{-3}	65.5±12.0	1.99±0.14	2.18×10^{-3}	1.41×10^{-5}

Kinetics of nucleotide insertion and chain extension reactions were determined as described in Materials and Methods. Frequencies of nucleotide insertion (F_{ins}) and chain extension (F_{ext}) were estimated by the following equation: $F=(V_{max}/K_m)$[wrong pair]/(V_{max}/K_m) [correct pair=dC:dG]. X=8-Br-dG lesion.

N.D., not detectable.

[a] Data were expressed as mean±SD obtained from three independent experiments.

by the 8-Br-dG and 8-Br-dA sites on their templates. As shown in Fig. 3a and b, the primer extension profiles of 8-Br-dG and 8-Br-dA were very similar and thus expected to show similar miscoding specificities between 8-Br-dG and 8-Br-dA. We determined both miscoding specificities by using two-phase PAGE (Fig. 2), and only 8-Br-dG had a miscoding potential (Fig. 4), and not 8-Br-dA (Supplementary Fig. S1). Therefore, the miscoding specificities of 8-Br-dG and 8-Br-dA are quite different even though their primer extension profiles are similar.

Little is known about the mutation spectrum induced by reactive brominating species, except for the miscoding spectrum of 5-Br-dU lesion, which has been reported in detail.[15] In this work, the miscoding spectra of 8-Br-dG, 8-Br-dA, and 5-Br-dC lesions were quantitatively determined in primer extension reactions in the presence of all four dNTPs. Among the DNA adducts, we found that only 8-Br-dG was a mutagenic lesion. When pol α was used, one-base deletion was detected opposite the lesion. In reactions catalyzed by pol κ, one-base deletion was observed, accompanied by lower

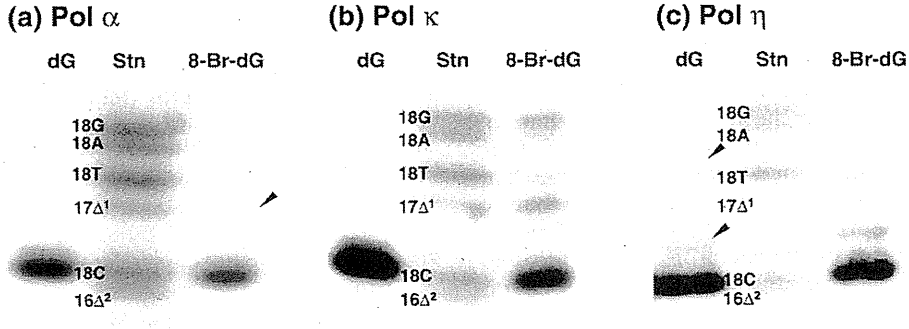

Fig. 4. Miscoding specificities of 8-Br-dG lesion in reactions catalyzed by pols α, κ, and η. Using unmodified and 8-Br-dG-modified 38-mer templates primed with an Alexa546-labeled 10-mer, we conducted primer extension reactions at 25 °C for 30 min in a buffer containing four dNTPs (100 μM each) and pol α (2000 fmol for unmodified and 8-Br-dG-modified templates), pol κ (10 fmol for unmodified and 8-Br-dG-modified templates), or pol η (50 fmol for unmodified and 8-Br-dG-modified templates), as described in Materials and Methods. The extended reaction products (>26 bases long) produced on the unmodified and modified templates were extracted following 20% denaturing PAGE. The recovered oligodeoxynucleotides were annealed to the complementary unmodified 38-mer and cleaved with EcoRI restriction enzyme. The entire product from the unmodified and 8-Br-dG-modified templates was subjected to two-phase PAGE (20×65×0.05 cm). The mobilities of the reaction products were compared with those of 18-mer standards (Fig. 2) containing dC, dA, dG, or dT opposite the lesion and one-base (Δ^1) or two-base (Δ^2) deletions.

amounts of dGMP, dAMP, and dTMP misincorporation (Fig. 4b). Thus, 8-Br-dG can pair with all the wrong bases at low frequency. This indicates that the broad mutation spectrum of 8-Br-dG may be generated in cells at the inflamed site. The spectrum was also supported by the steady-state kinetic studies (Table 1).

We revealed that both 8-Br-dA and 5-Br-dC adducts showed no miscoding events during *in vitro* DNA synthesis catalyzed by pols α, κ, and η. With respect to 8-Br-dA, all pols exclusively inserted dTMP, the correct base, opposite the lesion (Fig. S1). As the representative example of C8-dA DNA adducts, 8-oxo-7,8-dihydro-2′-deoxyadenosine also promoted the incorporation of dTMP, the correct base, in a similar two-phase PAGE system.[24] In contrast, 8-Br-dG and 8-oxo-7,8-dihydro-2′-deoxyguanosine (8-Oxo-dG), as C8-dG DNA adducts, promoted primary one-base deletion (Fig. 4) and misincorporation of dAMP,[25,26] respectively. Thus, we suggest that the miscoding potential of C8-dG adducts may be stronger than that of C8-dA adducts.

Moreover, we found that 5-Br-dC was also a nonmutagenic lesion. Pols α, κ, and η exclusively incorporated dGMP opposite the adduct (Fig. S1). However, 5-Br-dC may be converted to the thymidine analogue 5-Br-dU by deamination in cells. 5-Br-dU in the genomic DNA is paired with dA in the keto form and/or with dG in the enol form, which causes the mutations.[14,15] Thus, 5-Br-dC may cause the mutation via conversion to 5-Br-dU. On the basis of the current study, we suggest that 8-Br-dA and 5-Br-dC themselves are nonmutagenic DNA adducts.

Asahi *et al.* recently reported that the formation of 8-Oxo-dG and 8-Br-dG in LPS-treated rats was assessed by liquid chromatography–tandem mass spectrometry.[5] The study showed that the basal level of 8-Br-dG in the hepatic DNA and urine of the rats was at least 3 orders of magnitude lower than that of 8-Oxo-dG. Furthermore, the excretion of 8-Br-dG into the urine in the LPS-treated rats occurred earlier than for 8-Oxo-dG, implying that DNA repair of 8-Br-dG is more efficient than that of 8-Oxo-dG. In the present study, as shown in Table 2, the $F_{ins} \times F_{ext}$ ratio for the dG:8-Br-dG/dC:8-Br-dG pairs was 0.08. This number was remarkably lower than that for the dA:8-Oxo-dG/dC:8-Oxo-dG pairs (ratio = 1453). Similar results were observed with pol κ. The ratio of $F_{ins} \times F_{ext}$ past 8-Br-dG was at least 2 orders of magnitude lower than that of 8-Oxo-dG, indicating that the miscoding potential of 8-Br-dG was weaker than that of 8-Oxo-dG.[25,26] Overall, the miscoding potential, formation level, and accumulativeness in DNA of the 8-Br-dG adduct are lower than those of 8-Oxo-dG. Therefore, the contribution to mutagenesis at the inflamed site of 8-Br-dG may be limited.

Table 2. $F_{ins} \times F_{ext}$ past DNA adducts by mammalian DNA pols α and κ

	X=	8-Br-dG[a]	8-Oxo-dG[b,c]
Pol α	C:X	7.16×10^{-5}	1.70×10^{-5}
	A:X	N.D.	**2.47×10^{-2}**
	G:X	**5.48×10^{-6}**	N.D.
	T:X	N.D.	N.D.
Pol κ	C:X	3.00×10^{-3}	6.21×10^{-4}
	A:X	8.55×10^{-6}	**2.00×10^{-2}**
	G:X	**3.56×10^{-4}**	7.65×10^{-8}
	T:X	1.41×10^{-5}	5.98×10^{-5}

Values in boldface indicate a primarily misincorporated base opposite the DNA adduct.
N.D., not detectable.
[a] Data were taken from Table 1.
[b] Data for pol α were taken from Ref. 25.
[c] Data for pol κ were taken from Ref. 29.

In conclusion, two-phase PAGE analysis and steady-state kinetic studies were performed to determine the miscoding specificities of the brominated DNA lesions 8-Br-dG, 8-Br-dA, and 5-Br-dC. Among them, only 8-Br-dG, and not 5-Br-dC and 8-Br-dA, is a mutagenic lesion; the miscoding frequency and specificity vary depending on the DNA pol used. Thus, HOBr-induced 8-Br-dG adducts may contribute to mutagenic events at the site of inflammation.

Materials and Methods

Materials

Ultrapure dNTPs were from GE Healthcare. EcoRI restriction endonuclease was purchased from New England BioLabs. Blue Dextran was obtained from Sigma-Aldrich. Human pol α (1200 units/mg of protein) was purchased from CHIMERx (Milwaukee, WI). Human pol η was kindly provided by Drs. Chikahide Masutani and Fumio Hanaoka. Human pol κ was prepared as C-terminal truncations with 10 His-tags as previously described.[27]

Preparation of oligodeoxynucleotides

All oligodeoxynucleotides, Alexa546-labeled primers, standard markers, and site-specifically 8-Br-dG-, 8-Br-dA-, and 5-Br-dC-modified template were obtained from Japan Bio Service Co. (Saitama, Japan). Alexa546 was conjugated at the 5′-terminus of primers and standard markers. A single brominated DNA adduct was located at the 20th position from the 5′-termini in the modified 38-mer template (5′-CATGCTGATGAATTCCTTCXCTTCTTTCCTCTCCCTTT, where X represents 8-Br-dG, 8-Br-dA, or 5-Br-dC). The oligomers were purified by 20% denaturing PAGE before use. We demonstrated that the 8-Br-dG-, 8-Br-dA-, and 5-Br-dC-modified oligomers were stable at 25 °C for at least 6 h.

Primer extension reactions

Primer extension reactions catalyzed by pols α, κ, and η were conducted at 25 °C for 30 min in a buffer (10 μL) containing all four dNTPs (100 μM each) using 8-Br-dG-, 8-Br-dA-, and 5-Br-dC-modified and unmodified 38-mer templates (750 fmol) primed with an Alexa546-labeled 10-mer (500 fmol, 5′-AGAGGAAAGA) (Fig. 2). The reaction buffer for pol α contains 40 mM Tris–HCl (pH 8.0), 5 mM $MgCl_2$, 60 mM KCl, 10 mM dithiothreitol, 250 μg/mL bovine serum albumin, and 2.5% glycerol. The reaction buffer for pol η and pol κ contains 40 mM Tris–HCl (pH 8.0), 5 mM $MgCl_2$, 10 mM dithiothreitol, 250 μg/mL bovine serum albumin, 60 mM KCl, and 2.5% glycerol. The reaction was stopped by the addition of 2 μL of formamide dye containing Blue Dextran (100 mg/mL) and ethylenediaminetetraacetic acid (50 mM) and incubation at 95 °C for 3 min. The whole amount of the reaction sample was subjected to 20% denaturing PAGE (30 × 40 × 0.05 cm). The separated products were visualized by using Molecular Imager FX Pro and Quantity One software (Bio-Rad Laboratories). We demonstrated that the linear range to quantitatively detect fluorescent-labeled oligomers was from 5 to 1500 fmol.[21]

Quantitation of miscoding specificities and frequencies

Using 8-Br-dG-modified and unmodified 38-mer oligodeoxynucleotides (750 fmol) primed with an Alexa546-labeled 10-mer (500 fmol, 5′-AGAGGAAAGA), we conducted primer extension reactions catalyzed by pol α (2000 fmol), pol κ (10 fmol), or pol η (50 fmol) at 25 °C for 30 min in a buffer (10 μL) containing all four dNTPs (100 μM each) and subjected them to 20% denaturing PAGE (30 × 40 × 0.05 cm). Extended reaction products (>26 bases long) were extracted from the gel. The recovered oligodeoxynucleotides were annealed with the unmodified 38-mer, cleaved with EcoRI, and subjected to two-phase PAGE (20 × 65 × 0.05) containing 7 M urea in the upper phase and no urea in the middle and bottom phases (each phase containing 18%, 20%, and 24% polyacrylamide, respectively). The phase width is approximately 10, 37, and 18 cm from the upper phase. To quantify base substitutions and deletions, we compared the mobility of the reaction products with those of Alexa546-labeled 18-mer standards containing dC, dA, dG, or dT opposite the lesion and one-base (Δ^1) or two-base (Δ^2) deletions (Fig. 2).[19–21]

Steady-state kinetic studies of nucleotide insertion and extension

Kinetic parameters associated with nucleotide insertion opposite the 8-Br-dG lesion and chain extension from the 3′ primer terminus were determined at 25 °C, using varying amounts of single dNTPs. For insertion kinetics, reaction mixtures containing dNTP (0–500 μM) and either pol α (50–1000 fmol) or pol κ (10 fmol) were incubated at 25 °C for 0.5–5 min in 10 μL of Tris–HCl buffer (pH 8.0) using a 38-mer template (750 fmol) primed with an Alexa546-labeled 12-mer (500 fmol; 5′-AGAGGAAAGAAG). To measure chain extension, reaction mixtures containing a 38-mer template (750 fmol) primed with an Alexa546-labeled 13-mer (500 fmol; 5′-AGAGGAAAGAAGN, where N is C, A, G, or T), with varying amounts of dGTP (0–500 μM) and either pol α (25–1000 fmol) or pol κ (10 fmol), were used. The reaction samples were subjected to 20% denaturing PAGE (30 × 40 × 0.05). The Michaelis constant (K_m) and maximum rate of reaction (V_{max}) were determined with Enzyme Kinetics Module 1.1 of SigmaPlot 2001 software (SPSS Inc.). The frequencies of dNTP insertion (F_{ins}) and chain extension (F_{ext}) were determined relative to the dC:dG base pair according to the following equation:[28,29]

$$F = (V_{max}/K_m)_{[\text{wrong pair}]} / (V_{max}/K_m)_{[\text{correct pair = dC:dG}]}$$

Supplementary materials related to this article can be found online at doi:10.1016/j.jmb.2011.01.005

Acknowledgements

We are grateful to Drs. Fumio Hanaoka and Chikahide Masutani for providing human pol η. We thank Ms. Nagisa Kamoshita for assistance during the experiment. This research was supported in part by Grants-in-Aid for Scientific Research (22710068) from the Ministry of Education, Culture, Sports, Science and Technology. This work was also partially supported by Health, Welfare, and Labor Science Research Grants (H21-food-general-009 and H21-food-general-012) from the Japan Health Science Foundation.

References

1. Lewis, J. G. & Adams, D. O. (1987). Inflammation, oxidative DNA damage, and carcinogenesis. *Environ. Health Perspect.* **76**, 19–27.
2. Rothenberg, M. E. (1998). Eosinophilia. *N. Engl. J. Med.* **338**, 1592–1600.
3. Weiss, S. J., Test, S. T., Eckmann, C. M., Roos, D. & Regiani, S. (1986). Brominating oxidants generated by human eosinophils. *Science*, **234**, 200–203.
4. Henderson, J. P., Byun, J., Williams, M. V., McCormick, M. L., Parks, W. C., Ridnour, L. A. & Heinecke, J. W. (2001). Bromination of deoxycytidine by eosinophil peroxidase: a mechanism for mutagenesis by oxidative damage of nucleotide precursors. *Proc. Natl Acad. Sci. USA*, **98**, 1631–1636.
5. Asahi, T., Kondo, H., Masuda, M., Nishino, H., Aratani, Y., Naito, Y. *et al.* (2010). Chemical and immunochemical detection of 8-halogenated deoxyguanosines at early stage inflammation. *J. Biol. Chem.* **285**, 9282–9291.
6. Shen, Z., Mitra, S. N., Wu, W., Chen, Y., Yang, Y., Qin, J. & Hazen, S. L. (2001). Eosinophil peroxidase catalyzes bromination of free nucleosides and double-stranded DNA. *Biochemistry*, **40**, 2041–2051.

7. Thukkani, A. K., Albert, C. J., Wildsmith, K. R., Messner, M. C., Martinson, B. D., Hsu, F. F. & Ford, D. A. (2003). Myeloperoxidase-derived reactive chlorinating species from human monocytes target plasmalogens in low density lipoprotein. *J. Biol. Chem.* **278**, 36365–36372.
8. Gaut, J. P., Yeh, G. C., Tran, H. D., Byun, J., Henderson, J. P., Richter, G. M. *et al.* (2001). Neutrophils employ the myeloperoxidase system to generate antimicrobial brominating and chlorinating oxidants during sepsis. *Proc. Natl Acad. Sci. USA*, **98**, 11961–11966.
9. Mayeno, A. N., Curran, A. J., Roberts, R. L. & Foote, C. S. (1989). Eosinophils preferentially use bromide to generate halogenating agents. *J. Biol. Chem.* **264**, 5660–5668.
10. Thomas, E. L., Bozeman, P. M., Jefferson, M. M. & King, C. C. (1995). Oxidation of bromide by the human leukocyte enzymes myeloperoxidase and eosinophil peroxidase. Formation of bromamines. *J. Biol. Chem.* **270**, 2906–2913.
11. Shen, Z., Wu, W. & Hazen, S. L. (2000). Activated leukocytes oxidatively damage DNA, RNA, and the nucleotide pool through halide-dependent formation of hydroxyl radical. *Biochemistry*, **39**, 5474–5482.
12. Pattison, D. I. & Davies, M. J. (2004). Kinetic analysis of the reactions of hypobromous acid with protein components: implications for cellular damage and use of 3-bromotyrosine as a marker of oxidative stress. *Biochemistry*, **43**, 4799–4809.
13. Henderson, J. P., Byun, J., Takeshita, J. & Heinecke, J. W. (2003). Phagocytes produce 5-chlorouracil and 5-bromouracil, two mutagenic products of myeloperoxidase, in human inflammatory tissue. *J. Biol. Chem.* **278**, 23522–23528.
14. Yu, H., Eritja, R., Bloom, L. B. & Goodman, M. F. (1993). Ionization of bromouracil and fluorouracil stimulates base mispairing frequencies with guanine. *J. Biol. Chem.* **268**, 15935–15943.
15. Morris, S. M. (1991). The genetic toxicology of 5-bromodeoxyuridine in mammalian cells. *Mutat. Res.* **258**, 161–188.
16. Henderson, J. P., Byun, J., Williams, M. V., Mueller, D. M., McCormick, M. L. & Heinecke, J. W. (2001). Production of brominating intermediates by myeloperoxidase. A transhalogenation pathway for generating mutagenic nucleobases during inflammation. *J. Biol. Chem.* **276**, 7867–7875.
17. Kawai, Y., Morinaga, H., Kondo, H., Miyoshi, N., Nakamura, Y., Uchida, K. & Osawa, T. (2004). Endogenous formation of novel halogenated 2′-deoxycytidine. Hypohalous acid-mediated DNA modification at the site of inflammation. *J. Biol. Chem.* **279**, 51241–51249.
18. Efrati, E., Tocco, G., Eritja, R., Wilson, S. H. & Goodman, M. F. (1999). "Action-at-a-distance" mutagenesis. 8-oxo-7, 8-dihydro-2′-deoxyguanosine causes base substitution errors at neighboring template sites when copied by DNA polymerase β. *J. Biol. Chem.* **274**, 15920–15926.
19. Shibutani, S. (1993). Quantitation of base substitutions and deletions induced by chemical mutagens during DNA synthesis *in vitro*. *Chem. Res. Toxicol.* **6**, 625–629.
20. Shibutani, S., Suzuki, N., Matsumoto, Y. & Grollman, A. P. (1996). Miscoding properties of 3,N^4-etheno-2′-deoxycytidine in reactions catalyzed by mammalian DNA polymerases. *Biochemistry*, **35**, 14992–14998.
21. Yasui, M., Suenaga, E., Koyama, N., Masutani, C., Hanaoka, F., Gruz, P. *et al.* (2008). Miscoding properties of 2′-deoxyinosine, a nitric oxide-derived DNA Adduct, during translesion synthesis catalyzed by human DNA polymerases. *J. Mol. Biol.* **377**, 1015–1023.
22. Clark, J. M., Joyce, C. M. & Beardsley, G. P. (1987). Novel blunt-end addition reactions catalyzed by DNA polymerase I of *Escherichia coli*. *J. Mol. Biol.* **198**, 123–127.
23. Terashima, I., Suzuki, N., Dasaradhi, L., Tan, C. K., Downey, K. M. & Shibutani, S. (1998). Translesional synthesis on DNA templates containing an estrogen quinone-derived adduct: N^2-(2-hydroxyestron-6-yl)-2′-deoxyguanosine and N^6-(2-hydroxyestron-6-yl)-2′-deoxyadenosine. *Biochemistry*, **37**, 13807–13815.
24. Shibutani, S., Bodepudi, V., Johnson, F. & Grollman, A. P. (1993). Translesional synthesis on DNA templates containing 8-oxo-7,8-dihydrodeoxyadenosine. *Biochemistry*, **32**, 4615–4621.
25. Shibutani, S., Takeshita, M. & Grollman, A. P. (1991). Insertion of specific bases during DNA synthesis past the oxidation-damaged base 8-oxodG. *Nature*, **349**, 431–434.
26. Haracska, L., Prakash, L. & Prakash, S. (2002). Role of human DNA polymerase kappa as an extender in translesion synthesis. *Proc. Natl Acad. Sci. USA*, **99**, 16000–16005.
27. Niimi, N., Sassa, A., Katafuchi, A., Gruz, P., Fujimoto, H., Bonala, R. R. *et al.* (2009). The steric gate amino acid tyrosine 112 is required for efficient mismatched-primer extension by human DNA polymerase kappa. *Biochemistry*, **48**, 4239–4246.
28. Mendelman, L. V., Boosalis, M. S., Petruska, J. & Goodman, M. F. (1989). Nearest neighbor influences on DNA polymerase insertion fidelity. *J. Biol. Chem.* **264**, 14415–14423.
29. Mendelman, L. V., Petruska, J. & Goodman, M. F. (1990). Base mispair extension kinetics. Comparison of DNA polymerase alpha and reverse transcriptase. *J. Biol. Chem.* **265**, 2338–2346.

Mutation Research 725 (2011) 43–49

Contents lists available at ScienceDirect

Mutation Research/Genetic Toxicology and Environmental Mutagenesis

journal homepage: www.elsevier.com/locate/gentox
Community address: www.elsevier.com/locate/mutres

Induction of *TK* mutations in human lymphoblastoid TK6 cells by the rat carcinogen 3-chloro-4-(dichloromethyl)-5-hydroxy-2(5*H*)-furanone (MX)

Pasi Hakulinen*, Ayumi Yamamoto, Naoki Koyama, Wakako Kumita, Manabu Yasui, Masamitsu Honma

Division of Genetics and Mutagenesis, National Institute of Health Sciences, 1-18-1 Kamiyoga, Setagaya-ku, Tokyo 158-8501, Japan

ARTICLE INFO

Article history:
Received 18 October 2010
Received in revised form 25 May 2011
Accepted 29 June 2011
Available online 18 July 2011

Keywords:
MX
Loss of heterozygosity
LOH
TK gene mutation
Micronucleus test
Comet assay
TK6 cells

ABSTRACT

3-Chloro-4-(dichloromethyl)-5-hydroxy-2(5*H*)-furanone (MX), a chlorine disinfection by-product in drinking water, is carcinogenic in rats and genotoxic in mammalian cells *in vitro*. In the current study, the mechanism of genotoxicity of MX in human lymphoblastoid TK6 cells was investigated by use of the Comet assay, the micronucleus test, and the thymidine kinase (*TK*) gene-mutation assay. MX induced a concentration-dependent increase in micronuclei and *TK* mutations. The lowest effective concentrations in the MN test and the *TK* gene-mutation assay were 37.5 μM and 25 μM, respectively. In the Comet assay, a slight although not statistically significant increase was observed in the level of DNA damage induced by MX in the concentration range of 25–62.5 μM. Molecular analysis of the *TK* mutants revealed that MX induced primarily point mutations or other small intragenic mutations (61%), while most of the remaining *TK* mutants (32%) were large deletions at the *TK* locus, leading to the hemizygous-type loss-of-heterozygosity (LOH) mutations. These findings show that aside from inducing point mutations, MX also generates LOH at the *TK* locus in human cells and may thus cause the inactivation of tumour-suppressor genes by LOH.

1. Introduction

Epidemiological evidence indicates an association between life-time exposure to disinfection by-products (DBPs) in chlorinated drinking-water and an increased risk for cancer [1]. Of all the DBPs tested for carcinogenicity (~20 DBPs), 3-chloro-4-(dichloromethyl)-5-hydroxy-2(5*H*)-furanone (MX) is the most potent rodent carcinogen, producing tumours in multiple organs in rats [2]. In rat-liver epithelial cells, the target cells of MX-induced tumorigenicity in rats, MX causes DNA damage and gene mutations [3] and it also has tumour-promoting properties [4,5]. These studies together with others suggest that MX may be a complete carcinogen in rats. In the overall evaluation conducted by the International Agency for Research on Cancer (IARC), MX was designated as a group 2B carcinogen (possibly carcinogenic to humans) [1].

In spite of the extensive literature showing that MX is a potent genotoxicant in a wide variety of cell lines and endpoints *in vitro* [for a review, see 6], the primary mechanism of genotoxicity and animal tumorigenicity has remained unclear. MX has shown both clastogenic (sister chromatid exchange, chromosomal aberrations, micronuclei) and mutagenic properties. *In vitro*, MX induces point mutations (mainly GC→TA transversions) in *Salmonella typhimurium* strains [7–9] and at the hypoxanthine-phosphoribosyl transferase (*Hprt*) locus in Chinese hamster ovary (CHO) cells [10]. On the other hand, MX was not found to be mutagenic *in vivo*, in transgenic *gpt* delta mice [5]. Furthermore, analyses of mutations in the MX-induced rat liver tumours revealed no point mutations in *Ras* genes and only few point mutations in the *p53* gene [11]. The mechanism that initiates the MX-induced point mutations *in vitro* is unknown. DNA adducts are formed *in vitro* in the reaction of MX with nucleosides and calf-thymus DNA in buffer solutions [12–15], but there are no reports indicating that MX-induced DNA adducts are formed in bacteria or mammalian cells in culture or *in vivo*.

The aim of the present work was to study the genotoxic properties of MX in human lymphoblastoid TK6 cells. TK6 cells have been used in numerous mutation studies, because the *TK* gene-mutation assay detects not only intragenic events – mainly point mutations – but also loss of heterozygosity (LOH), which can result from large-scale chromosomal deletions, recombinations, and aneuploidy [16,17]. This feature makes the assay useful for evaluating the ability of chemicals to induce various mutational events. A major part of the genetic damages detected in *TK* mutants occur in human tumours and thus have relevance to carcinogenicity. In the present study, we investigated the capability of MX to induce *TK* mutants in TK6 cells and determined the types of mutation at the molecular level. In addition, we evaluated the ability of MX to induce DNA damage, analyzed by the use of Comet assay, and chromosomal damage, measured as micronuclei in the TK6 cells.

* Corresponding author. Present address: Department of Environmental Health, National Institute for Health and Welfare, P.O. Box 95, FI-70701 Kuopio, Finland. Tel.: +358 20 610 6455; fax: +358 20 610 6499.
E-mail address: pasi.hakulinen@thl.fi (P. Hakulinen).

1383-5718/$ – see front matter © 2011 Elsevier B.V. All rights reserved.
doi:10.1016/j.mrgentox.2011.07.004

2. Materials and methods

2.1. Cell growth and treatment

The human lymphoblastoid TK6 cell line was isolated by Skopek et al. [18] as a non-tumour, p53-proficient cell line, immortalized by Epstein-Barr virus. The cell line is heterozygous at the *thymidine kinase* (*TK*) locus and thus the remaining wild-type allele serves as the target for a recessive mutation. The cells were grown in RPMI-1640 medium (Nacalai Tesque Inc., Kyoto, Japan) containing 10% (v/v) heat-inactivated horse serum (SAFC Biosciences, Lenexa, KS), antibiotics (100 U/ml penicillin, 100 μg/ml streptomycin), and 200 μg/ml sodium pyruvate at 37 °C in an atmosphere of 5% CO_2.

3-Chloro-4-(dichloromethyl)-5-hydroxy-2(5*H*)-furanone (MX, CAS No. 77439-76-0) was from Wako Pure Chemical Industries Ltd. (Osaka, Japan). For the exposure of the cells to MX, 20 ml aliquots of the cell suspension at a concentration of 5.0×10^5 cells/ml were pipetted into 50-ml tubes (1 tube per concentration). MX (final concentrations: 6.25, 12.5, 25, 37.5, 50, and 62.5 μM) was added to the tubes in 200 μl of RPMI 1640 plus supplements. After 4 h of treatment at 37 °C with gentle shaking (26–27 rpm), 500 μl of the cell suspension was pipetted into a 1.5-ml microcentrifuge tube for the Comet assay. The remaining cells were centrifuged (1000 rpm, 5 min), washed, and re-suspended in 50 ml of fresh RPMI-1640 plus supplements. For the cell-viability study, the cells were diluted for plating into 96-well plates. For the micronucleus test and the *TK* gene-mutation assay, the cell suspensions were cultured in 75-cm^2 flasks. Thus, the assays were conducted with aliquots of the same batch of cells.

The assays were also performed in the presence of an exogenous metabolic activation system (rat liver S9).

2.2. Comet assay

The alkaline Comet assay (single-cell gel electrophoresis, SCGE) was carried out according to the method of Singh et al. [19]. Briefly, 500 μl of treated cell suspension was centrifuged, the cells were washed and suspended in 1 ml of Hank's balanced salt solution (HBSS) supplemented with 20 mM Na_2EDTA and 10% DMSO. A suspension of cells was mixed with 0.5% NuSieve® GTG® Agarose (Cambrex Bio Science Rockland Inc., Rockland, ME) and spread on a microscope slide (Matsunami Glass Ind. Ltd., Osaka, Japan) coated with 1% agarose GP-42 (Nakalai Tesque Inc.), and covered with 0.5% agarose-LGT. The agarose was allowed to solidify for 5 min at room temperature. The cells were lysed at 4 °C overnight in 2.5 M NaCl, 100 mM Na_2EDTA, 10 mM Tris, 10% DMSO, 1% Triton X-100, pH 10. The following day, slides were transferred to an electrophoresis chamber filled with the ice-cold solution of 0.3 M NaOH, 1 mM EDTA at pH > 13 for 20 min to allow the DNA to unwind. Then electrophoresis was carried out for 15 min at 300 mA. Finally, the slides were neutralized for 5 min in 0.4 M Tris buffer (pH 7.5). Analysis of the Comets was done on SYBR® Gold stained slides (100 cells analyzed per concentration) using the Comet assay IV (Perceptive Instruments Ltd., UK) image-analysis system. The Comet response-parameter used in the statistical analysis was tail intensity (% of DNA migrating into the tail).

2.3. Micronucleus test

The micronucleus test was conducted 48 h after treatment. Approximately 10^6 cells were suspended in hypotonic solution (0.075 M KCl), and then fixed in two steps (2 × 5 min) in ice-cold fixative solution (methanol:acetic acid, 3:1). Finally, the cells were suspended in methanol containing 1% acetic acid. A drop of the cell suspension was spotted on a glass slide and air-dried. The slides were stained with 40 μg/ml acridine orange solution just before microscopic observation. A total of at least 1000 intact interphase cells per concentration were analyzed for the presence of micronuclei by use of a fluorescence microscope.

2.4. TK gene-mutation assay

For the measurement of plating efficiency (PE_0) on day 0 after exposure, the TK6 cells were plated into wells of a 96-well plate (1.6 cells/0.2 ml/well). After 14 days of incubation at 37 °C in an atmosphere of 5% CO_2, the colonies were scored. For the determination of mutation frequency (MF) ($TK^{-/-}$ mutants per 10^6 viable cells) after exposure, the TK6 cells were transferred into the 75-cm^2 flasks and maintained in logarithmic growth for three days to permit expression of the *TK*-deficient phenotype. The cell suspensions were diluted to below 3×10^5 cells/ml each day to prevent overgrowth. At the end of the expression period, the cell density was adjusted to 2×10^5 cells/ml in 50 ml of growth medium. For the *TK*-deficient mutant selection (containing the recessive mutation), the cells were cloned into 96-well plates at 40,000 cells/well in growth medium (0.2 ml) in the presence of the selective agent trifluorothymidine (TFT, final concentration 3 μg/ml). Cells were also seeded at a density of 1.6 cells/well into 96-well plates in the absence of TFT to determine plating efficiency (PE). The plates were incubated at 37 °C in an atmosphere of 5% CO_2 for 14 days. Then the colonies in the PE and TFT plates (normally growing (NG) *TK* mutants) were scored. The plates containing TFT were then re-fed with TFT at a final concentration of 30 μg/ml. After re-feeding, the plates were incubated for another 14 days, and again the colonies (slowly growing (SG) *TK* mutants) were scored. Cytotoxicity for the TK6 cells was evaluated as relative survival (RS) calculated from PE_0 and relative suspension growth (RSG), derived from cell growth-rate during a 3-day expression period.

2.5. Analysis of loss of heterozygosity

For the determination of loss of heterozygosity (LOH) an independent experiment was done with MX at 37.5 μM. After a 4-h exposure, the TK6 cells were washed and re-suspended in 20 ml of growth medium. Cells were transferred into 25-cm^2 flasks and incubated for 3 days (37 °C, 5% CO_2). For the *TK*-deficient mutant selection, the cells were then fed with TFT (final concentration 3 μg/ml) and cloned into 96-well plates. After 14 days of incubation (37 °C, 5% CO_2), the NG mutants were transferred from 96-well to 24-well plates in growth medium containing 3 μg/ml TFT, in order to expand the number of cells. The cells in the 96-well plates containing TFT were re-fed with TFT (final concentration 30 μg/ml) and incubated for an additional 14 days. After incubation, the SG mutants were also transferred from 96- to 24-well plates with 3 μg/ml TFT. The NG and SG mutant clones were also tested for growth in medium containing CHAT (deoxycytidine, hypoxanthine, aminopterin, and thymidine), which reduces the number of background mutants. Clones were classified as mutants if they were sensitive to CHAT but able to grow in the presence of TFT. The 24-well plates were incubated for 1–2 weeks (37 °C, 5% CO_2) followed by transfer of the cells into 25-cm^2 flasks. The cells were cultured for 1–2 weeks until the number of *TK* mutant cells was high enough ($1–2 \times 10^6$ cells) to extract genomic DNA, which was done with the Puregene® Genomic DNA Purification Kit (Gentra Systems, Minneapolis, MN). PCR was performed for those parts of exons 4 and 7 of the human *TK* gene that were heterozygous for frameshift mutations. β-Globin was used as the internal control. For the determination of LOH, a microsatellite locus on chromosome 17q was also subjected to PCR amplification. The PCR products were analyzed with an ABI PRISM® 3100-Avant™ Genetic Analyzer (PE Applied Biosystems, Chiba, Japan) and classified into three classes: non-LOH, hemizygous LOH (hemi-LOH), or homozygous LOH (homo-LOH) mutants. The results were processed by ABI PRISM® GeneMapper™ software v3.5 (PE Applied Biosystems) according to the manufacturer's guidelines. For the additional determination of the extent of LOH at the *TK* locus of TK6 cells, 10 microsatellite regions (D17S799, THRA, D17S1299, D17S855, D17S588, D17S807, D17S789, D17S785, D17S802, and D17S784) were analyzed on chromosome 17 by means of multiple PCR reactions and ABI PRISM® 3100-Avant™ Genetic Analyzer, and GeneMapper™ software v3.5.

2.6. Statistics

Three independent experiments were conducted in each assay. Statistical analyses were done on the combined data of the experiments. Levene's test for equality of variances was used for all the responses and, consequently, a parametric or a non-parametric test was chosen. The analysis of variance (ANOVA) followed by Dunnett's *post hoc* test was used for the analysis of data from the *TK* gene-mutation assay and the cytotoxicity test. The results of the micronucleus test and the Comet assay were analyzed with the non-parametric Kruskall–Wallis test. *P*-values ≤ 0.05 were considered statistically significant. The data were analyzed with the PASW statistics version 18.0 (SPSS Inc., Chicago, IL).

3. Results

3.1. Cytotoxicity and genotoxicity of MX

The TK6 cells were treated with various concentrations of MX for 4 h. The results of cytotoxicity and genotoxicity assays are presented in Fig. 1. Two parameters were used to assess the cytotoxicity of MX: relative survival (RS) and relative suspension growth (RSG). RS is the plating efficiency immediately after exposure, whereas RSG is the relative cell growth during the three days following treatment. For the *TK* gene-mutation assay, the highest concentration of the test chemical should cause 10–20% RS or RSG [20]. Over the concentration range used, MX evoked a concentration-dependent reduction in cell viability, permitting 9.5% RS and 14.9% RSG at the maximum concentration of 62.5 μM.

The Comet assay was conducted to assess the induction of DNA damage in TK6 cells. The test concentrations used covered the range from maximum acceptable toxicity to little or no toxicity in the assay [21]. A concentration-related positive trend was observed for the DNA-damaging effect of MX in TK6 cells, but the effect was not statistically significant (Kruskall–Wallis test).

Genotoxic effects of MX were also evaluated with the micronucleus test and the *TK* gene-mutation assay. Exposure to MX increased the number of micronuclei (MN) and *TK* mutants in TK6 cells in a concentration-related fashion (Fig. 1). The induction of

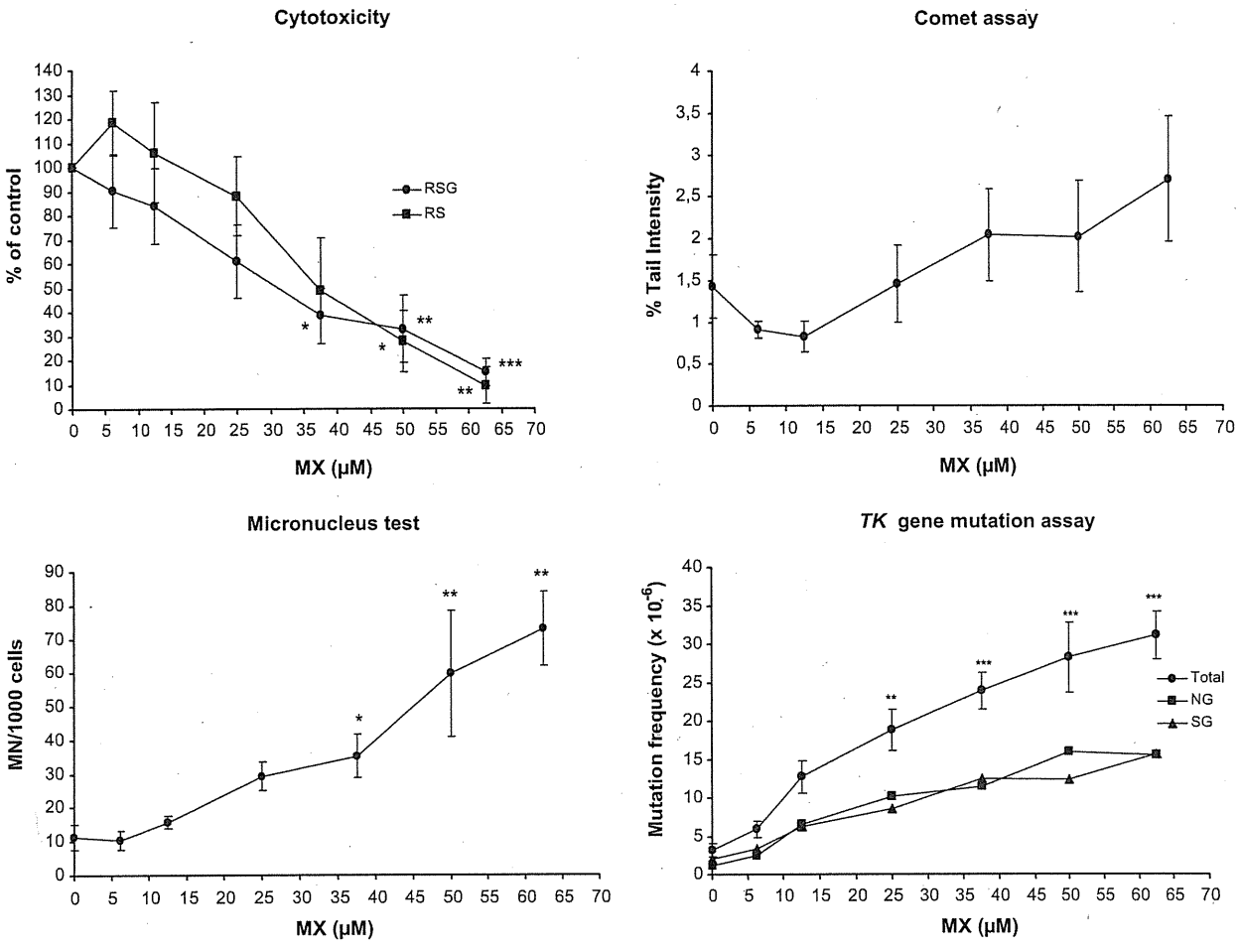

Fig. 1. Cytotoxic (relative survival, RS; relative suspension growth, RSG) and genotoxic responses (Comet assay, micronucleus test, and *TK* gene-mutation assay) in TK6 cells exposed to MX for 4 h (three experiments, mean values ± SEM). Asterisks indicate statistically significant differences with the negative control $^{*}P \leq 0.05$, $^{**}P \leq 0.01$, and $^{***}P \leq 0.001$ (Kruskall–Wallis test for Comet assay and micronucleus test, and ANOVA followed by Dunnett's *post hoc* test for *TK* gene-mutation assay and cytotoxicity test).

MN and *TK* mutants was statistically significant from 37.5 μM and 25 μM, respectively. Even concentrations that were not strongly cytotoxic induced both MN and *TK* mutants. At the highest concentration (62.5 μM), the potencies of MX to induce MN and *TK* mutations were 6.5 and 9.7 times the control level, respectively.

Two distinct phenotypic classes of *TK* mutants were generated in the assay. Normally growing (NG) mutants proliferate with a growth rate similar to that of the wild-type cells (doubling time, 13–17 h), and slowly growing (SG) mutants grow with doubling time of >21 h. NG mutants are generally the result of small intragenic mutations (point mutations, small deletions and insertions), while SG mutants result from gross structural changes involving a putative growth-regulating gene near the *TK* gene [17]. The NG and SG mutants induced by MX were almost equal in number (Fig. 1 and Table 1).

Methyl methanesulfonate (MMS) was used as a positive control chemical in the assays (30 μg/ml for the Comet assay and 5 μg/ml for the micronucleus test and the *TK* gene-mutation assay). MMS produced a positive response in each assay: Comet assay; % tail intensity: 42.2; micronucleus test: 74.7 MN/1000 cells; *TK* mutation frequency ($TK^{-/-}$ mutants per 10^6 viable cells): 47.9

The assays were also performed in the presence of a rat-liver exogenous metabolic activation system (S9 mix). Fig. 2 shows the data obtained from one independent experiment. In the presence of S9 mix no increases in the induction of DNA damage, frequency of MN, or *TK* mutants were detected at any MX concentration tested. S9 mix enhanced the activity of cyclophosphamide (5 μg/ml), the positive control chemical: cytotoxicity: 22.3% RS and 21.6% RSG; micronucleus test: 85 MN/1000 cells; *TK* mutation frequency: 28×10^{-6}.

3.2. Molecular analyses of TK mutants

The *TK* mutants were independently isolated from the cells treated with 37.5 μM MX for 4 h. The *TK* mutation frequency for

Table 1
LOH analysis of normally growing (NG) and slowly growing (SG) *TK* mutants induced by MX.

	Number of *TK* mutants	Non-LOH	Hemi-LOH	Homo-LOH
Spontaneous[a]				
NG mutants	19	14 (74%)	3 (16%)	2 (11%)
SG mutants	37	0 (0%)	9 (24%)	28 (76%)
Total	56	14 (25%)	12 (21%)	30 (54%)
37.5 μM MX				
NG mutants	70	68 (97%)	2 (3%)	0 (0%)
SG mutants	60	11 (18%)	40 (67%)	9 (15%)
Total	130	79 (61%)	42 (32%)	9 (7%)

[a] Data from Zhan et al. [22].

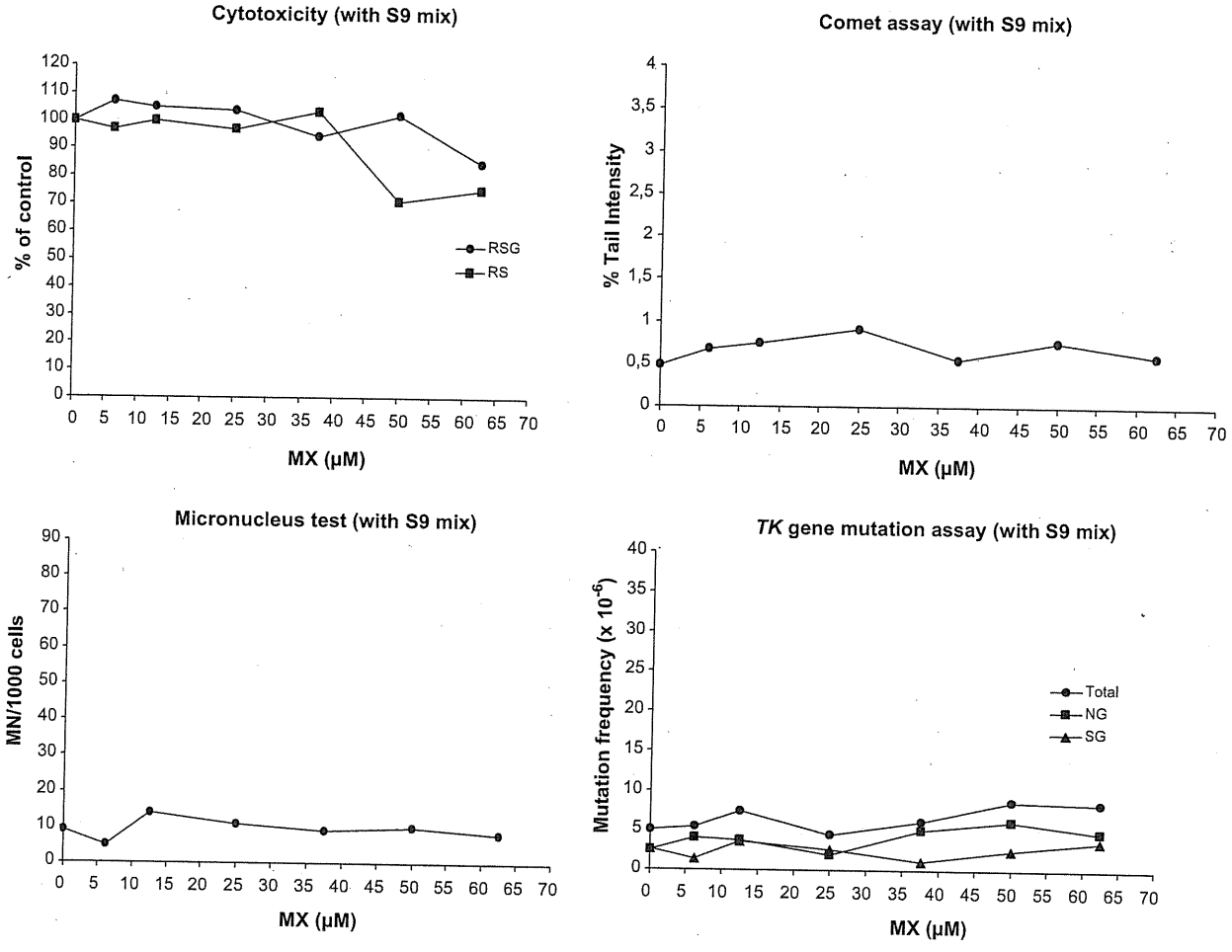

Fig. 2. Cytotoxic (relative survival, RS; relative suspension growth, RSG) and genotoxic responses (Comet assay, micronucleus test, and *TK* gene-mutation assay) in TK6 cells exposed to MX for 4 h with metabolic activation (S9 mix) (one experiment).

37.5 μM MX was about 5-fold higher than the concurrent control. The cytotoxic responses were 82% RS and 66.8% RSG. A total of 130 MX-induced *TK* mutants (70 NG and 60 SG mutants) were compared to those of spontaneously occurring *TK* mutants described previously [22] (Table 1). The numbers of NG and SG mutants analyzed depended on the ratio of NG and SG mutants in the assay. In this independent experiment, the proportion of SG mutants among the total number of *TK* mutants was lower compared with the combined data of the three experiments (Table 2). PCR-based loss of heterozygosity (LOH) analysis of genomic DNA from *TK* mutants was used to classify the mutants into non-LOH, hemizygous LOH (hemi-LOH) and homozygous LOH (homo-LOH). In general, non-LOH results from a small intragenic mutation (e.g., point mutation) in the *TK* gene, hemi-LOH from a chromosomal deletion (the functional *TK* allele is lost), and homo-LOH from inter-allelic homologous recombination (the functional *TK* allele is replaced by a non-functional *TK* allele) [17]. Most (61%) of the MX-induced *TK* mutants (NG and SG mutants) were of the non-LOH type (Table 1), indicating that MX predominantly induced point or other small intragenic mutations in TK6 cells. Three percent of NG and 82% of SG mutants resulted from LOH. Of those, all the NG and most of the SG mutants were hemi-LOH. Thus, deletion was a major event in the induction of LOH mutations in TK6 cells by MX. This is in contrast to spontaneous *TK* mutants, which were mainly homo-LOH (Table 1, reported previously [22]).

For a better illustration of the extent of LOH responsible for deletion and recombination at 10 microsatellite loci of chromosome 17, hemi-LOH and homo-LOH mutants are shown as bars in Fig. 3. Molecular analyses of MX-induced LOH mutants showed an extensive loss of functional *TK* sequences. In all of the MX-induced LOH events, the deleted or exchanged chromosome segment extended to the telomere.

Table 2
Total mutation frequencies (MF) and the proportion of slowly growing (SG) *TK* mutants induced by MX in the *TK* gene-mutation assay.

MX treatment (μM)	Mutational response	
	MF[a]	% SG
Combined data of the three experiments		
0	3.2	65.6
6.25	5.9	57.6
12.5	12.7	49.6
25	18.8	45.7
37.5	23.9	51.9
50	28.2	43.6
62.5	31.1	50.2
An independent experiment for the molecular analysis of *TK* mutants		
0	6.9	46.4
37.5	31.6	39.0

[a] $TK^{-/-}$ mutants per 10^6 viable cells.